# Six mrads and Two Endstations: Squeezing it all in at the GSECARS (13BM) Bending Magnet Beamlines

*Peter J. Eng*
*CARS*
*University of Chicago*

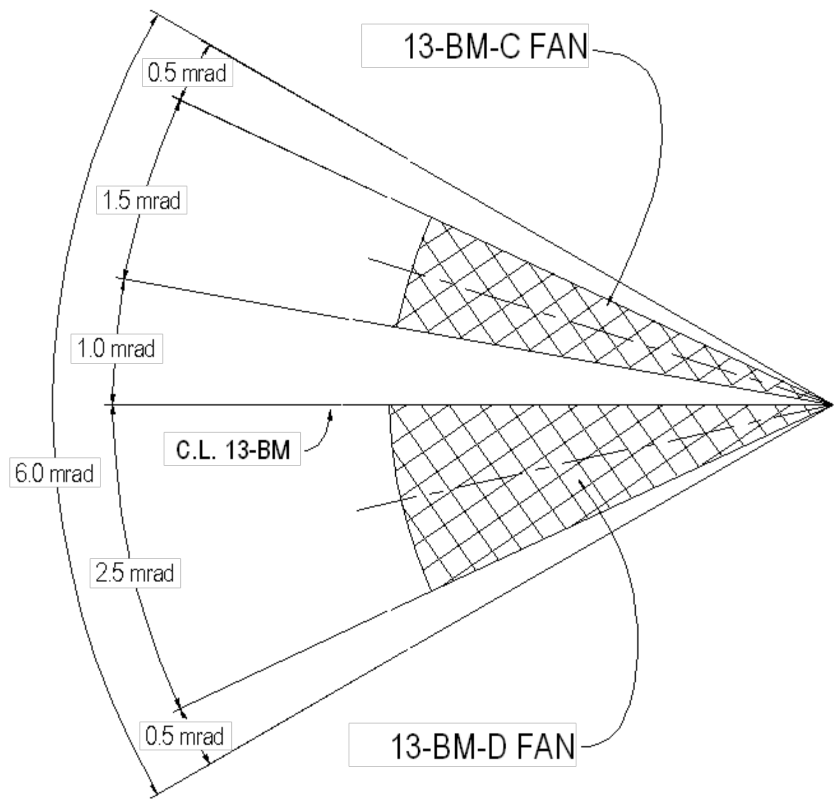

## APS BM Source

- 6 mrad of beam
- Excellent source of high-energy x-rays Ec =20 keV
- Small Source 65 x 275 um FWHM allows focusing to small spot sizes

## Only comparable high-energy x-ray source in US is X-17 NSLS

## Great Source for:

- High-pressure studies (DAC and LVP)
- Microcrystal Diffraction
- Microtomography / Radiography (Mono and Pink)
- Spectroscopy (EXAFS)
- XRF Microprobe
- Surface and Interface Scattering

## Two Independent Experiment Stations (can operate 100% of the time):

- 13-BM-C (side station)
  - Accepts up to1.5 mrad
  - Energy Range 7.5 – 30 keV (not scannable and monochromatic only)
- 13-BM-D (end station)
  - Accepts up to 2.5 mrad
  - Energy Range 5.6 – 70 keV (scannable, white and pink)

# GSECARS Sector 13

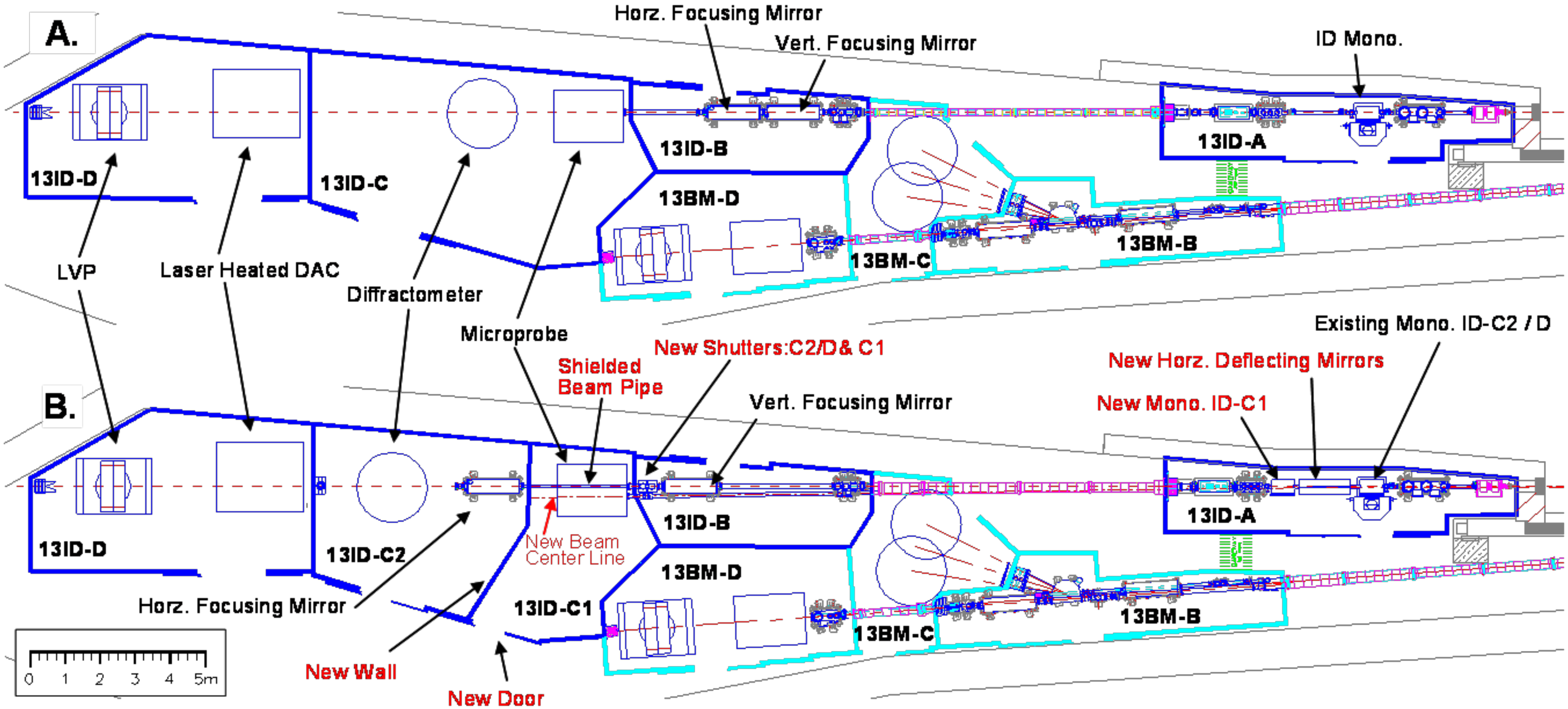


Figure 4-1. GSECARS sector 13 present single undulator layout (A) and proposed canted undulator mode (B).

# 13BM

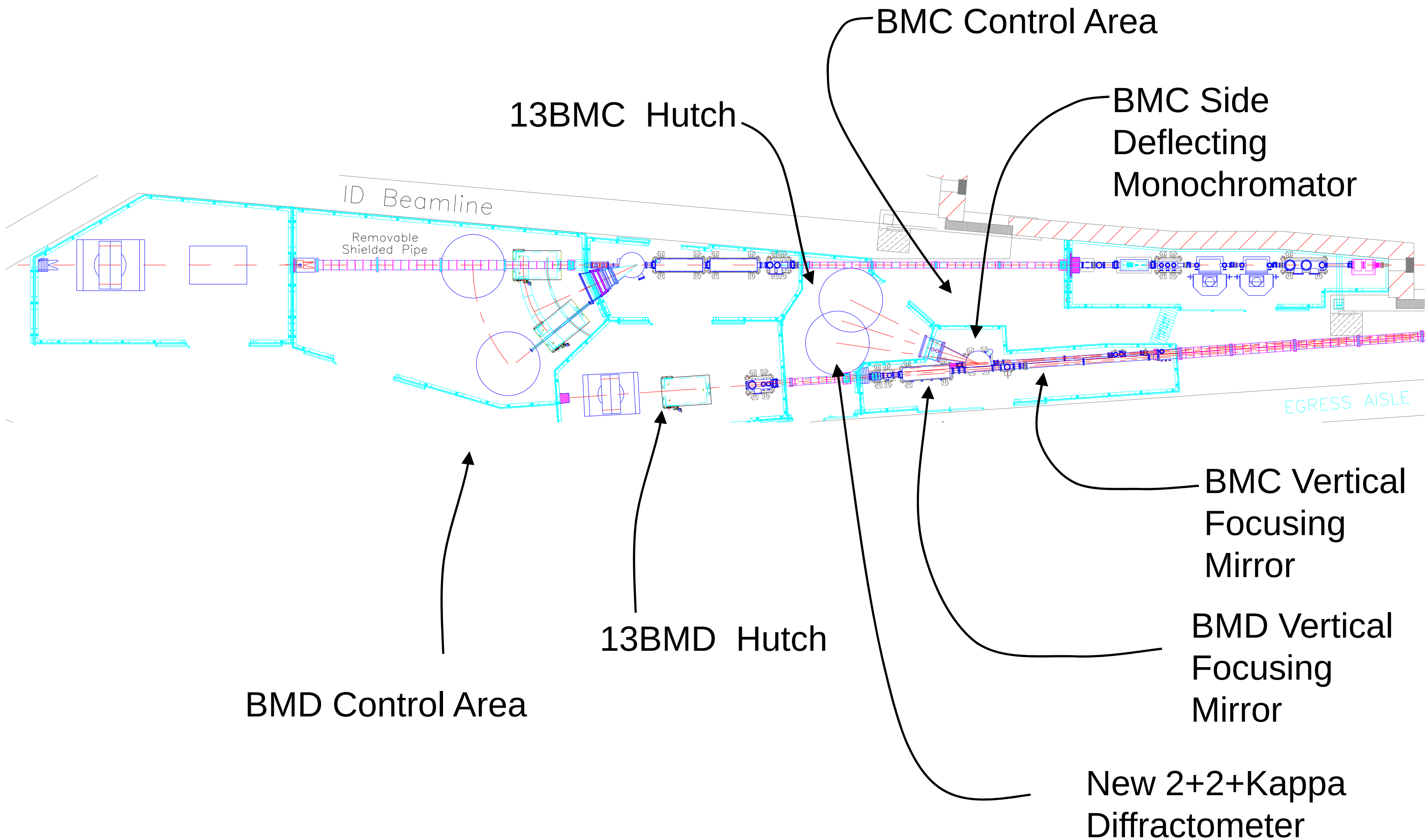
BMC Control Area
BMC Side Deflecting Monochromator
13BMC Hutch
ID Beamline
Removable Shielded Pipe
EGRESS AISLE
BMC Vertical Focusing Mirror
BMD Vertical Focusing Mirror
13BMD Hutch
BMD Control Area
New 2+2+Kappa Diffractometer

# 13BMC

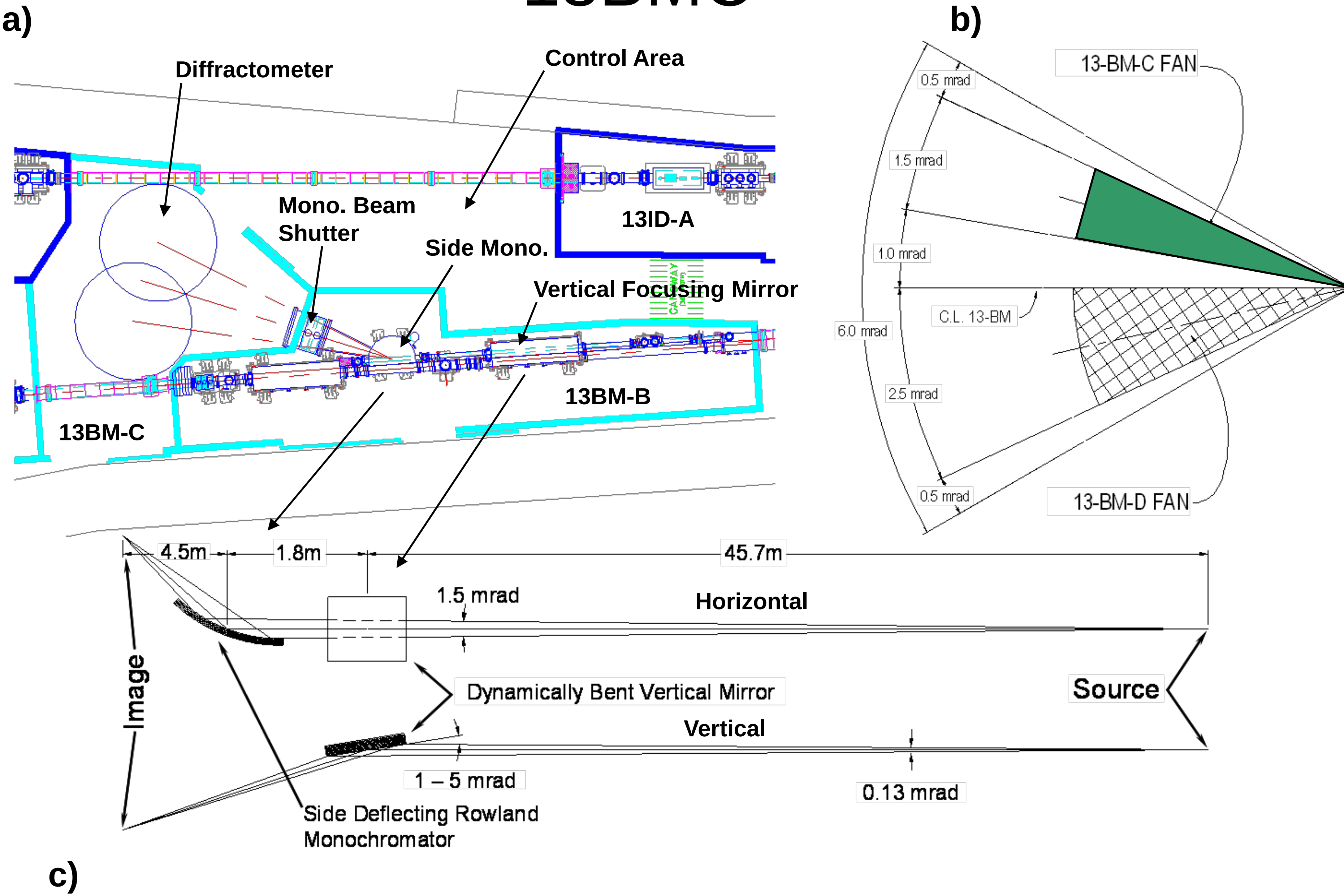

a)
Diffractometer
Control Area
Mono. Beam
Shutter
Side Mono.
13ID-A
Vertical Focusing Mirror
13BM-B
13BM-C
b)
13-BM-C FAN
0.5 mrad
1.5 mrad
1.0 mrad
6.0 mrad
C.L. 13-BM
2.5 mrad
0.5 mrad
13-BM-D FAN
4.5m
1.8m
45.7m
1.5 mrad
Horizontal
Image
Dynamically Bent Vertical Mirror
Source
Vertical
1 – 5 mrad
0.13 mrad
Side Deflecting Rowland
Monochromator
c)

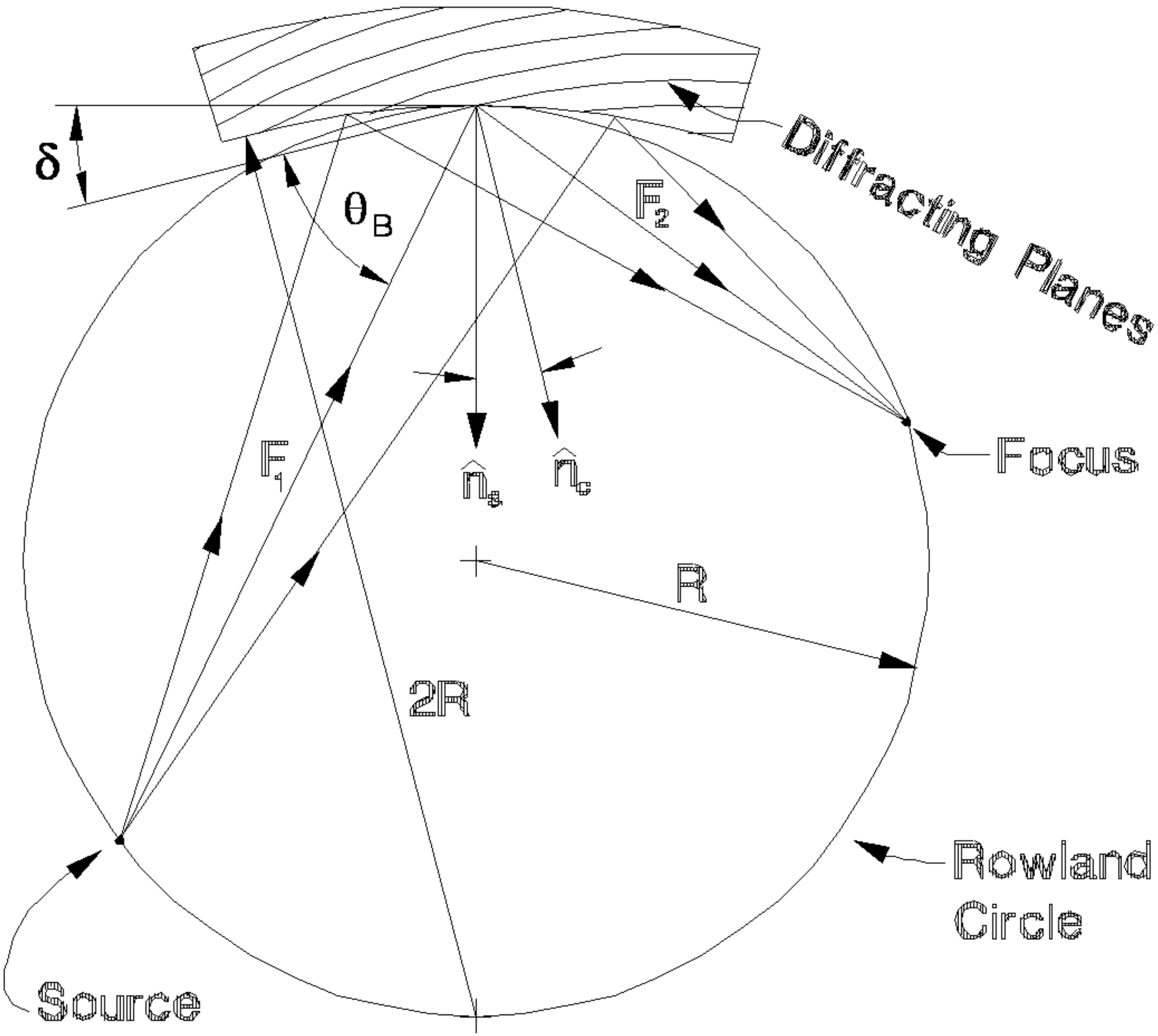
Diffracting Planes
δ
$\theta_B$
$F_2$
$F_1$
$\hat{n}_s$
$\hat{n}_c$
Focus
R
2R
Rowland Circle
Source

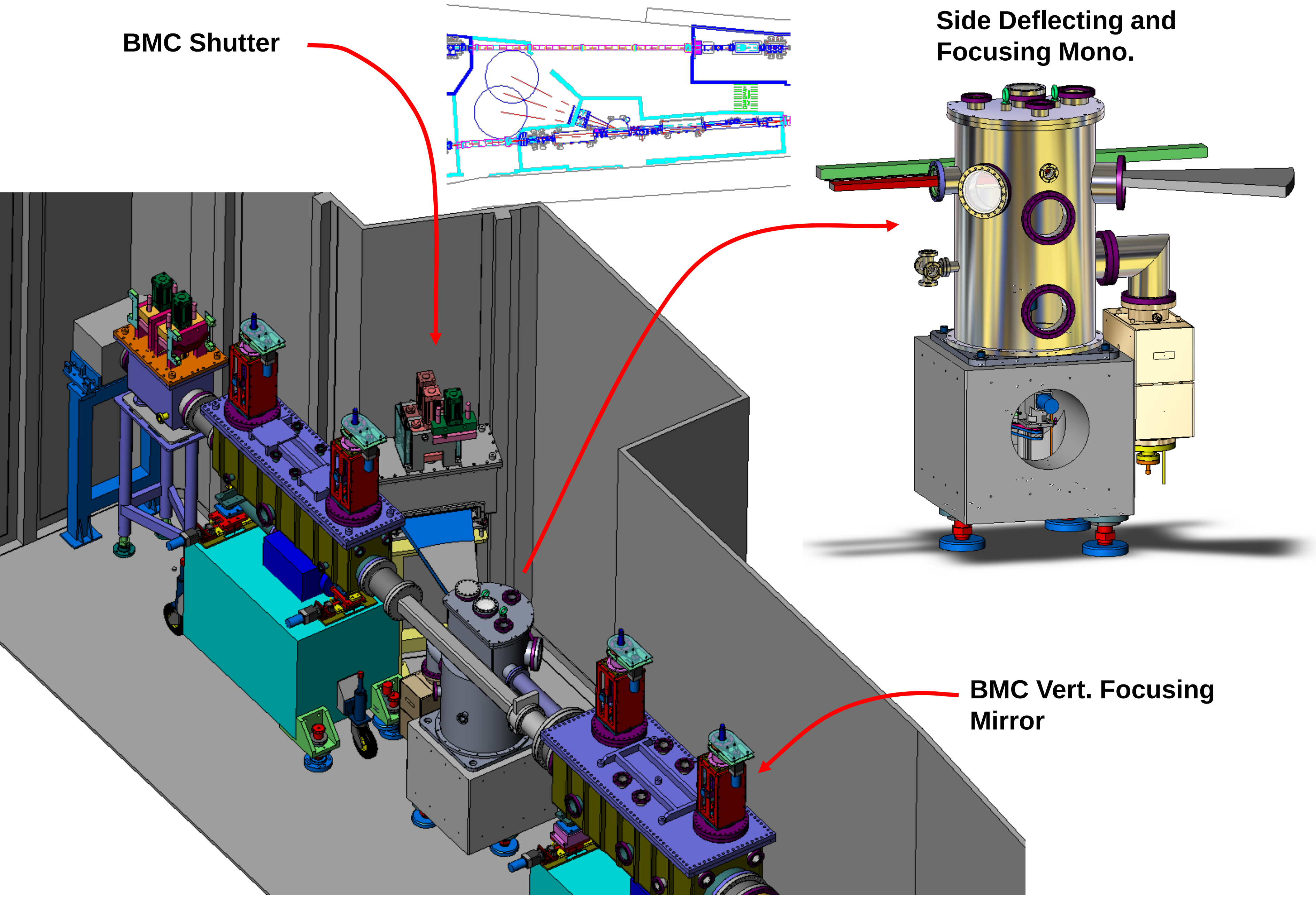
BMC Shutter
Side Deflecting and
Focusing Mono.
BMC Vert. Focusing
Mirror

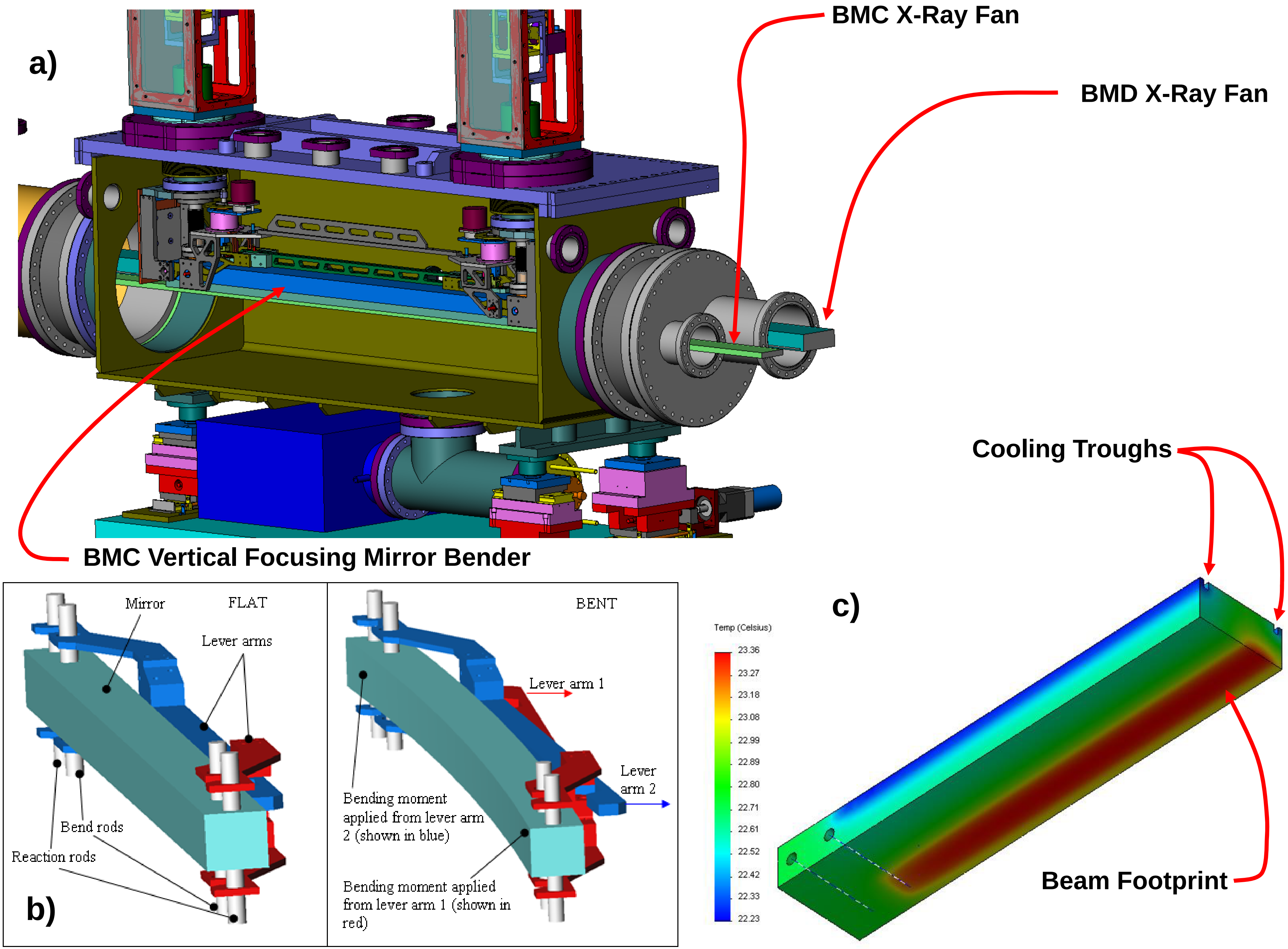
a)
BMC X-Ray Fan
BMD X-Ray Fan
BMC Vertical Focusing Mirror Bender
Cooling Troughs
b)
Mirror
FLAT
Lever arms
Bend rods
Reaction rods
BENT
Lever arm 1
Lever arm 2
Bending moment applied from lever arm 2 (shown in blue)
Bending moment applied from lever arm 1 (shown in red)
c)
Temp (Celsius)
23.36
23.27
23.18
23.08
22.99
22.89
22.80
22.71
22.61
22.52
22.42
22.33
22.23
Beam Footprint


HPS

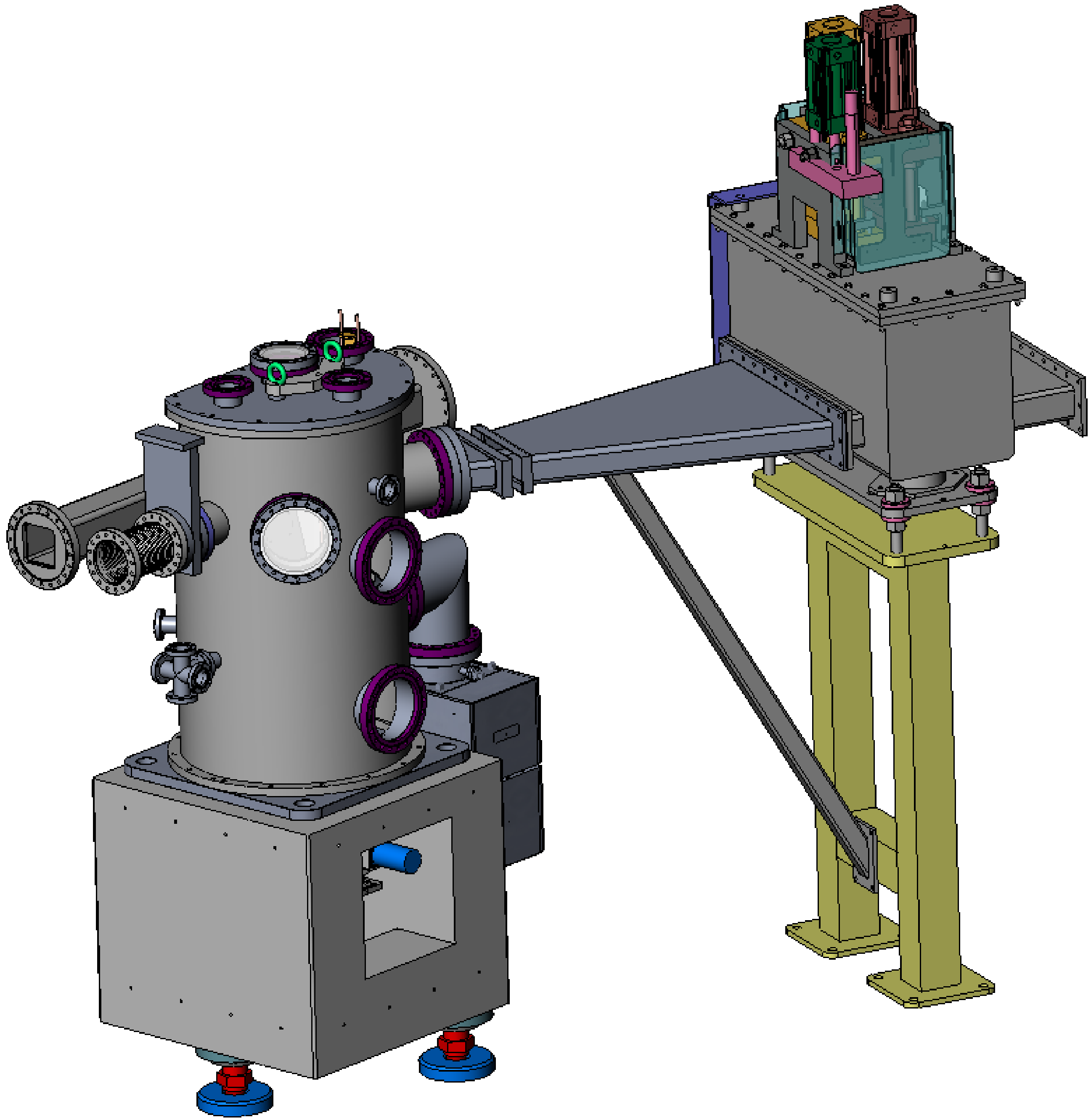

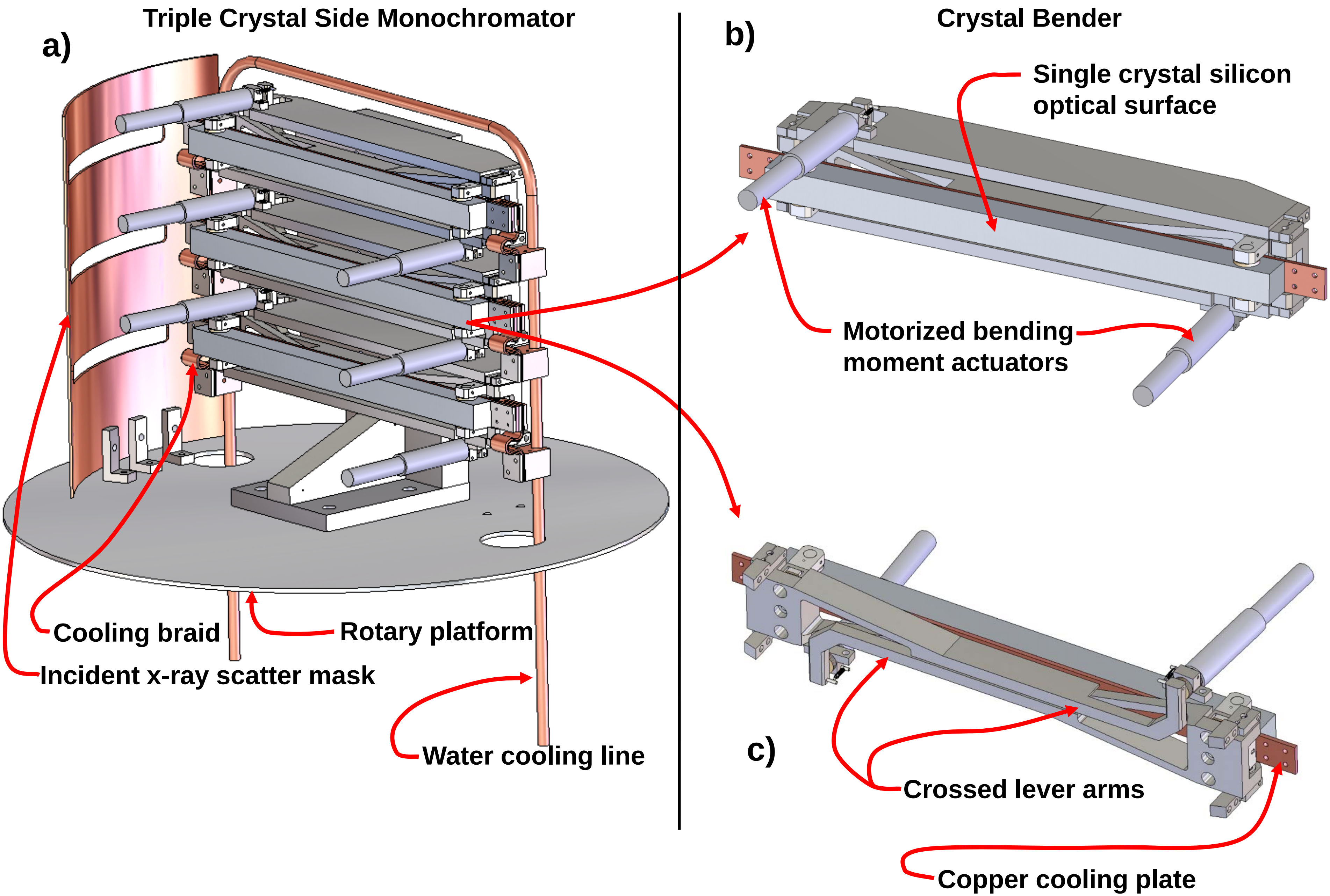
Triple Crystal Side Monochromator
a)
Crystal Bender
b)
Single crystal silicon optical surface
Motorized bending moment actuators
Cooling braid
Rotary platform
Incident x-ray scatter mask
Water cooling line
c)
Crossed lever arms
Copper cooling plate

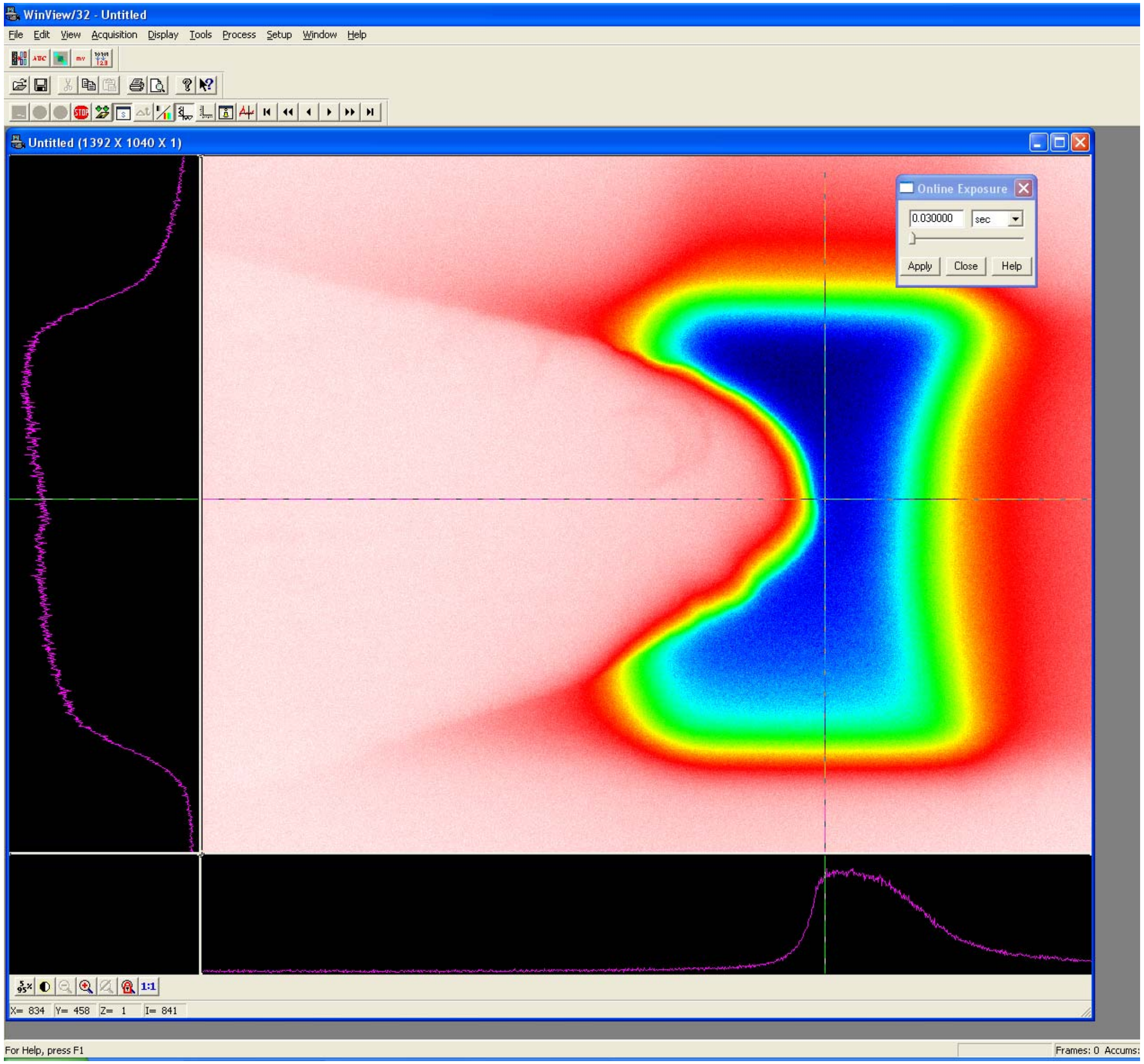
WinView/32 - Untitled
File Edit View Acquisition Display Tools Process Setup Window Help
Untitled (1392 X 1040 X 1)
Online Exposure
0.030000
sec
Apply
Close
Help
1:1
X= 834 Y= 458 Z= 1 I= 841
For Help, press F1
Frames: 0 Accums:

# Surface and Interface Scattering Stations – BMC – Optics

| Energy [keV] | Vertical Mirror Intercepts | Side Deflecting Mono. | Beam Size H x V [FWHM μm] | Beam Divergence H x V [FWHM mrad] | Total Flux [photons / sec] | Techniques Supported |
|---|---|---|---|---|---|---|
| 10 | 58% | Si (111) $\delta = 9.5^{o}$ $2\theta = 22.8^{o}$ | 23 x 28 | 15 x 0.55 | $1 \times 10^{12}$ | Surface and Interfaces; Microcrystallography |
| 18 | 61% | Si (111) $\delta = 5.2^{o}$ $2\theta = 12.6^{o}$ | 26 x 28 | 10 x 0.53 | $8 \times 10^{11}$ | Surface and Interfaces; Microcrystallography; DAC |
| 30 | 51% | Si (220) $\delta = 5.1^{o}$ $2\theta = 12.4^{o}$ | 26 x 28 | 10 x 0.32 | $5 \times 10^{11}$ | Microcrystallography; DAC |

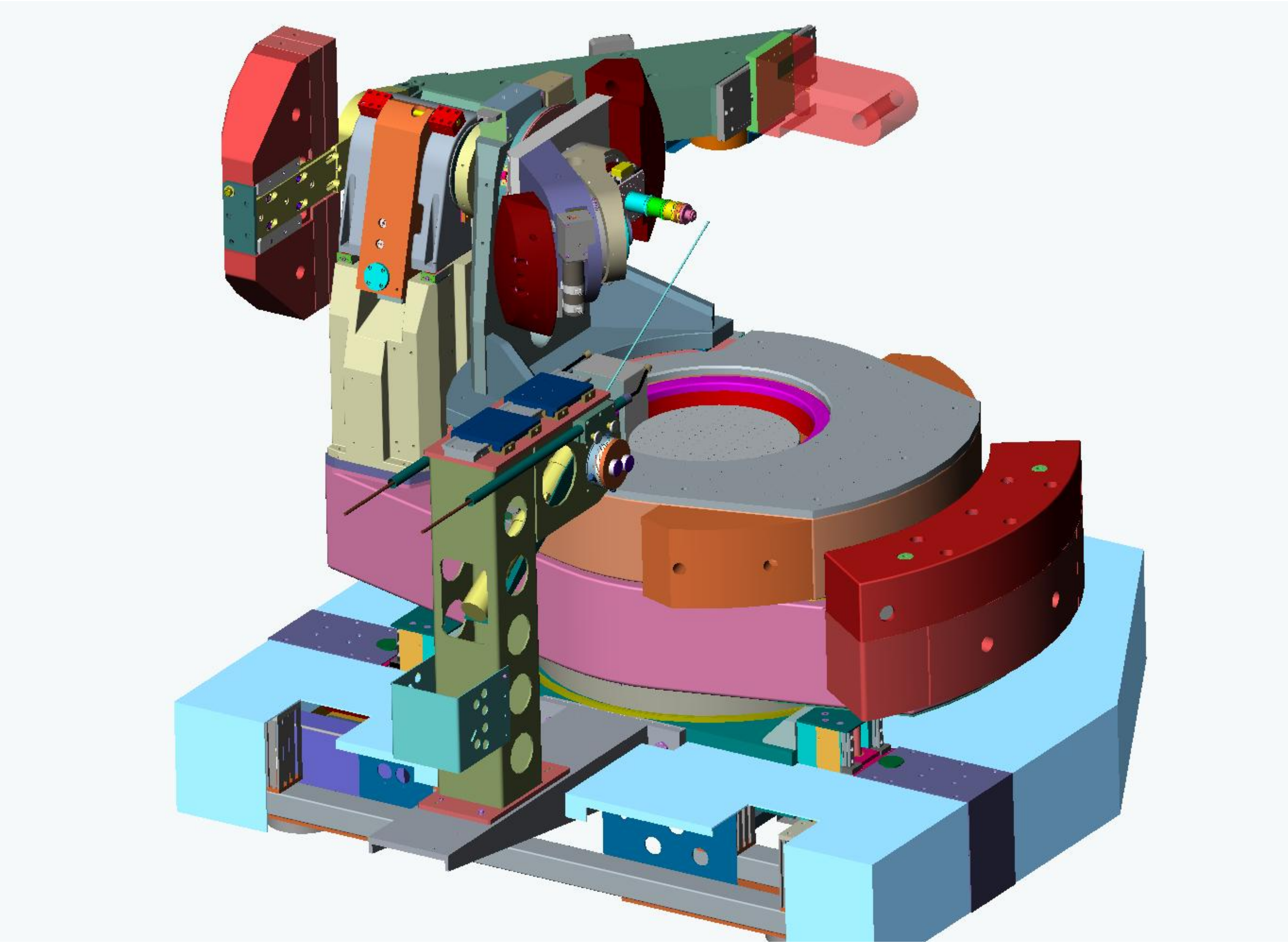

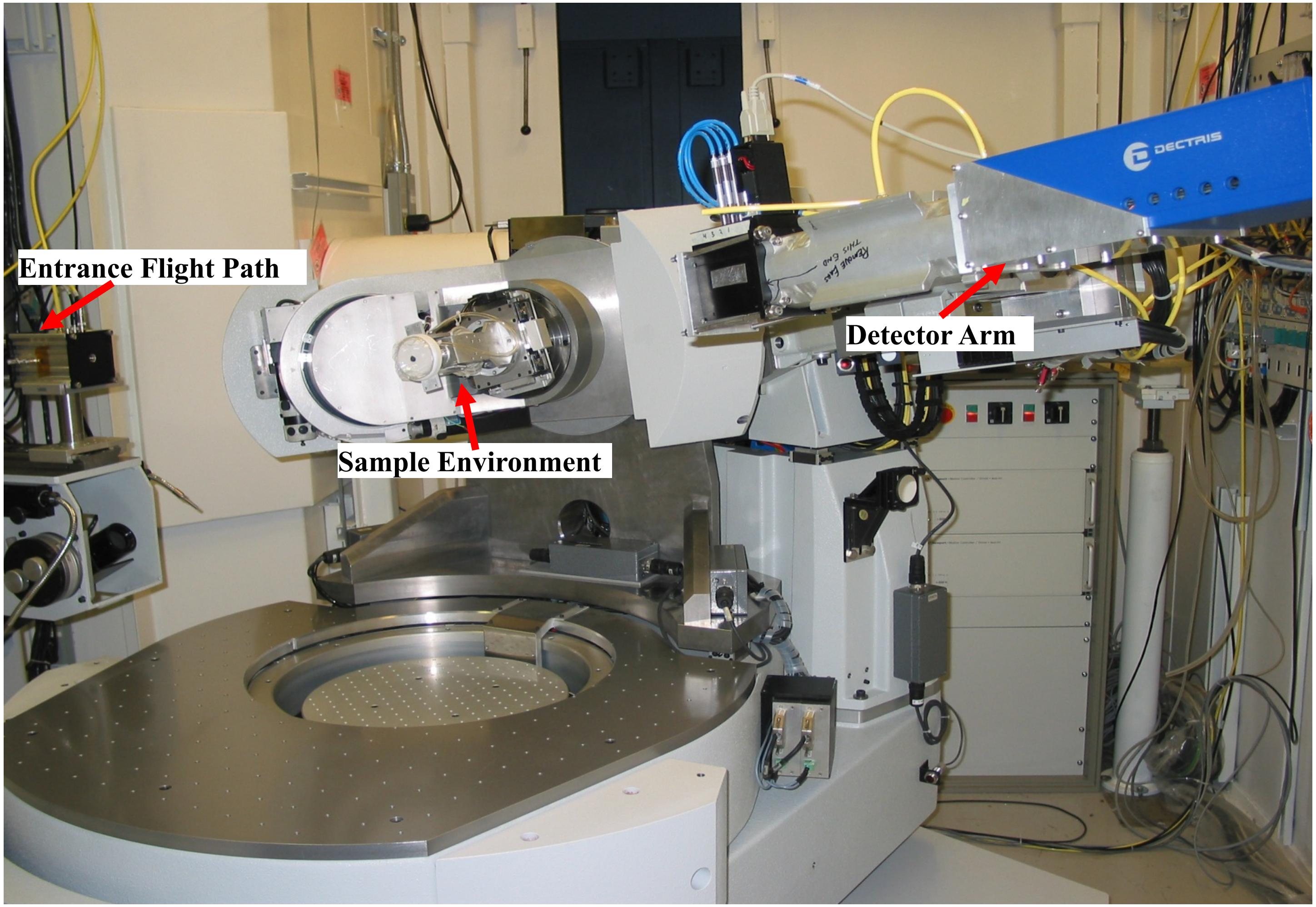
Entrance Flight Path
Sample Environment
Detector Arm
DECTRIS

- In-situ liquid cell with thin membrane.
  - Adjustable membrane gap for rapid changes in bulk chemistry and flow experiments.
  - Traps 1 μm or less of liquid for scattering and spectroscopy measurements.

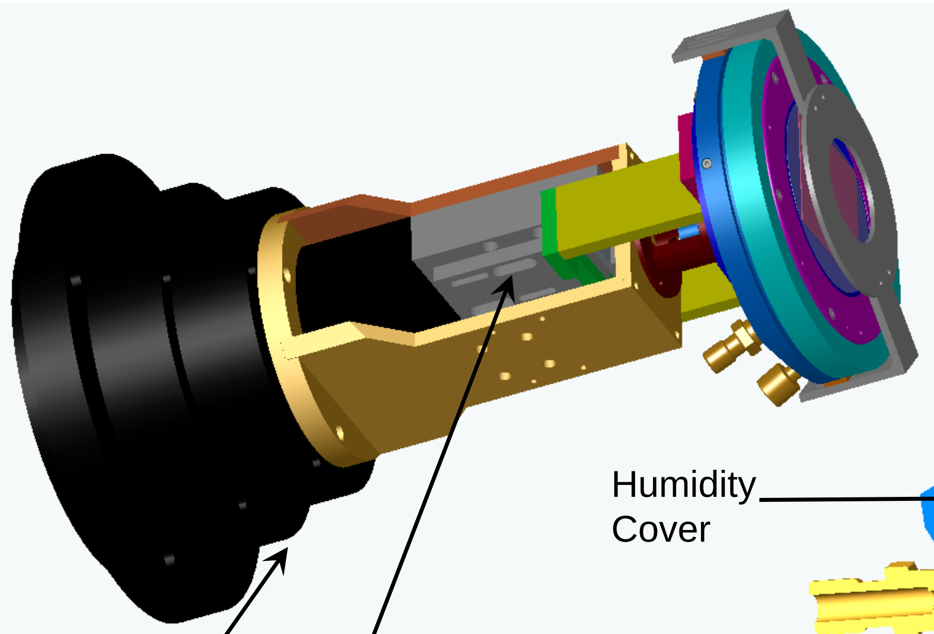


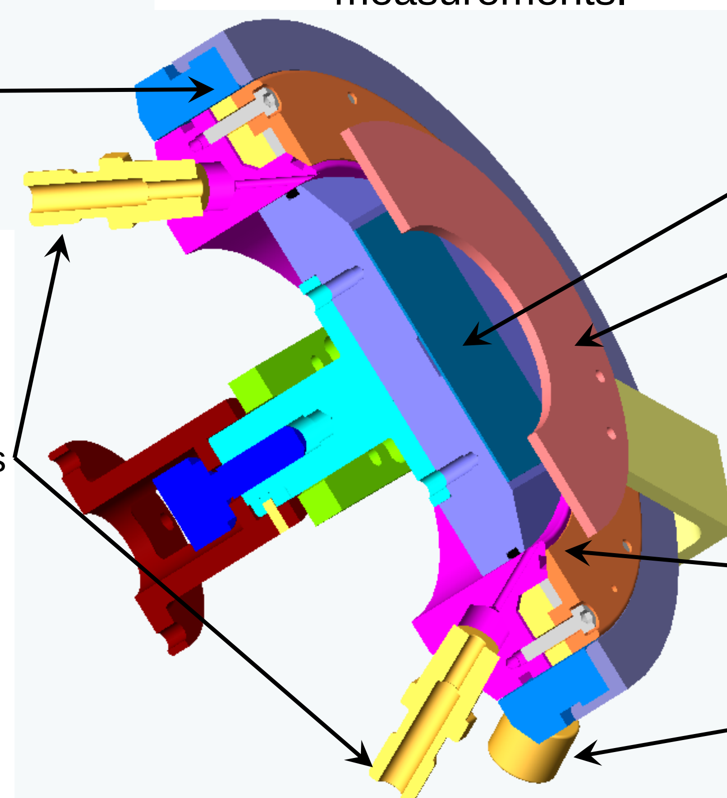


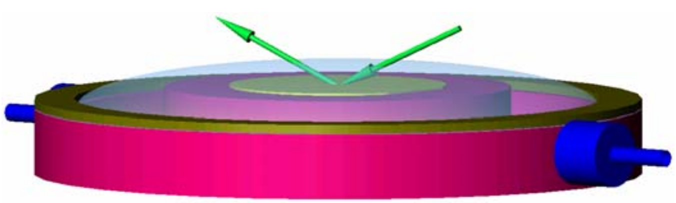

## Pixel Array Detector: " Pilatus 100K”

| | |
|---|---|
| **Pixel size** | **172 x 172 µm^2** |
| **Active area** | **83.8 x 33.5 x mm2** |
| **Counting rate** | **>2x10^6/pixel/s** |
| **Energy range** | **3 – 30 keV (abs. 100% - 10%)** |
| **Readout time** | **2.7 ms** |
| **Framing rate** | **200 Hz** |
| **Power consumption** | **15 W, air-cooled** |
| **Dimensions** | **275 x 146 x 85 mm** |
| **Weight** | **4 kg** |

http://www.dectris.com/sites/pilatus100k.html

# Pixel Array Detector and High Speed Trajectory Scanning

**SPEC scan for both STEP and TRAJECTORY SCANNING mode with the Newport XPS motor controller and Pilatus detector.**

**lup chi -2 2 1000 .015**

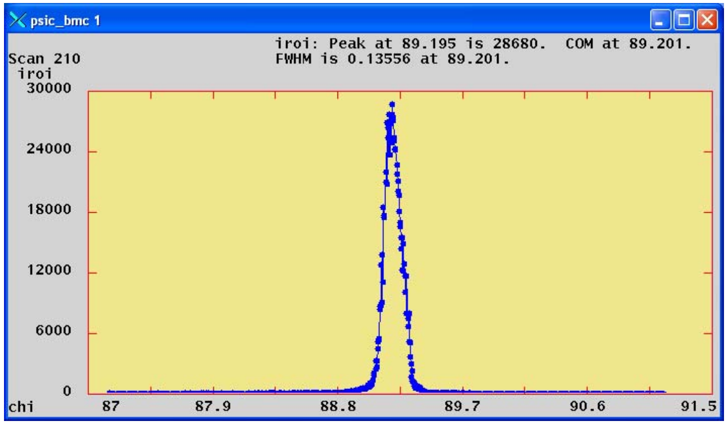


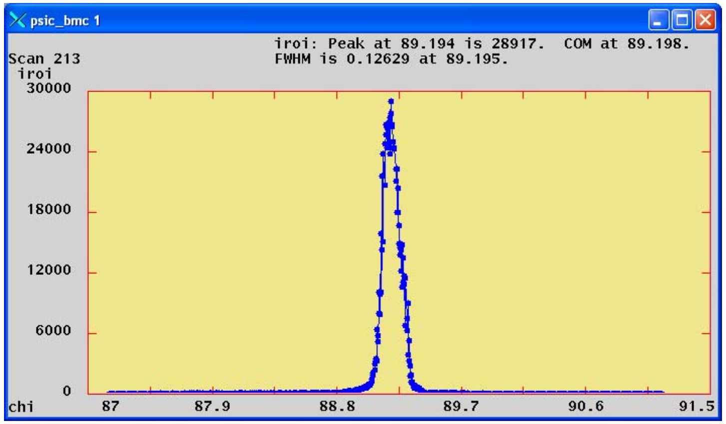


| SCAN TYPE | Total Time taken(seconds) |
|---|---|
| STEP | 870 |
| TRAJECTORY | 16.3 |

**Most of the overhead in STEP scan is the settling time for motors, with only a small fraction due to the Pilatus single exposure mode**

**TRAJECTORY SCANNING 50 times faster to execute the identical STEP SCAN**

# Pixel Array Detector: EPICS Support – 32 ROIs

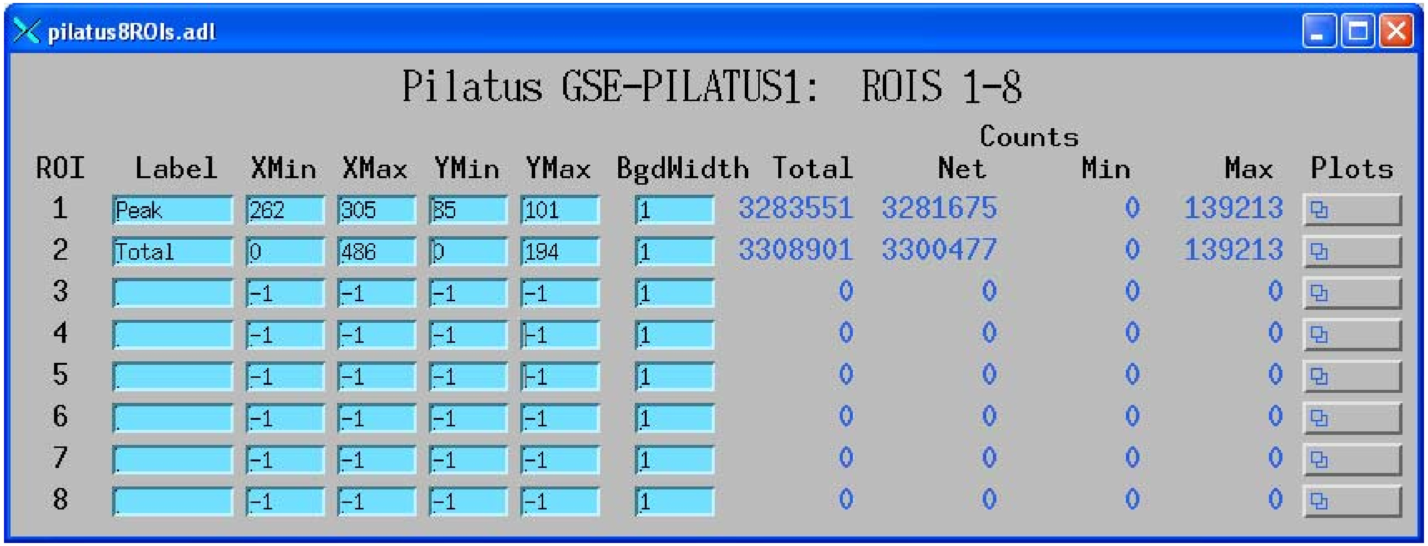

pilatus8ROIs.adl

Pilatus GSE-PILATUS1: ROIS 1-8

| ROI | Label | XMin | XMax | YMin | YMax | BgdWidth | Counts Total | Counts Net | Counts Min | Counts Max | Plots |
|---|---|---|---|---|---|---|---|---|---|---|---|
| 1 | Peak | 262 | 305 | 85 | 101 | 1 | 3283551 | 3281675 | 0 | 139213 | |
| 2 | Total | 0 | 486 | 0 | 194 | 1 | 3308901 | 3300477 | 0 | 139213 | |
| 3 | | -1 | -1 | -1 | -1 | 1 | 0 | 0 | 0 | 0 | |
| 4 | | -1 | -1 | -1 | -1 | 1 | 0 | 0 | 0 | 0 | |
| 5 | | -1 | -1 | -1 | -1 | 1 | 0 | 0 | 0 | 0 | |
| 6 | | -1 | -1 | -1 | -1 | 1 | 0 | 0 | 0 | 0 | |
| 7 | | -1 | -1 | -1 | -1 | 1 | 0 | 0 | 0 | 0 | |
| 8 | | -1 | -1 | -1 | -1 | 1 | 0 | 0 | 0 | 0 | |

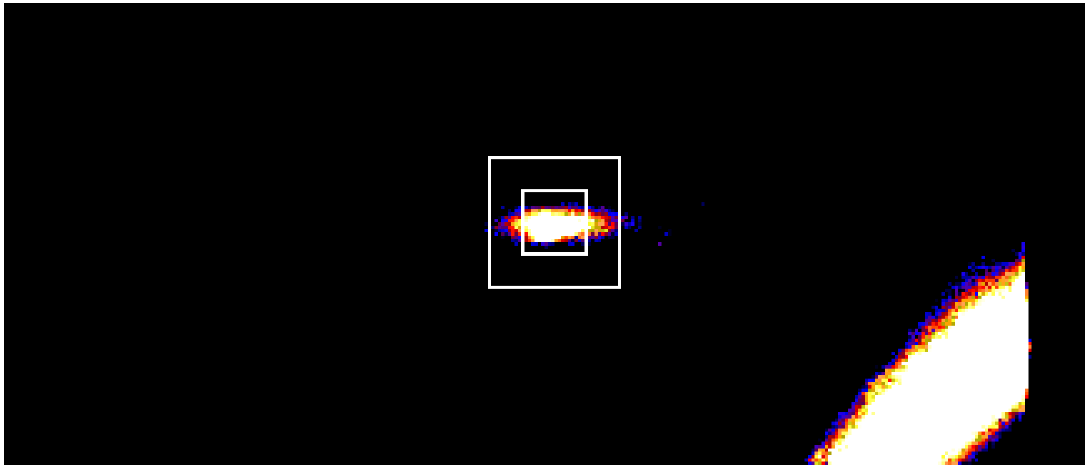

## (*11L*) rod profile for goethite(100)

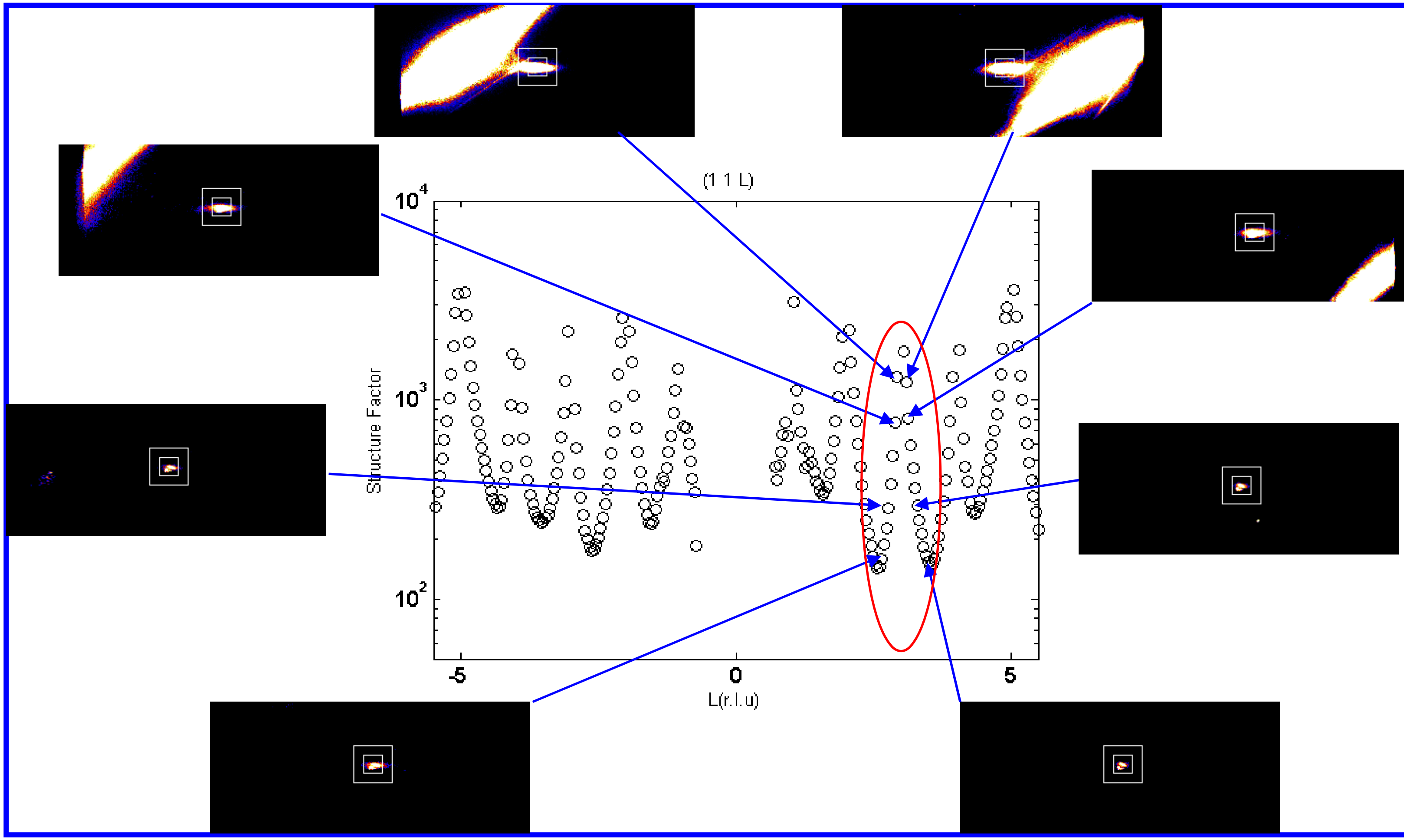

# Structure of goethite(100)/water interface

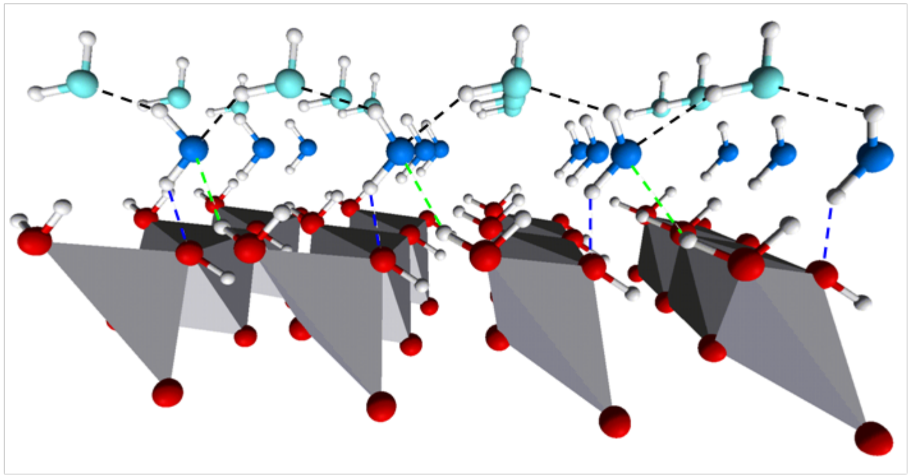

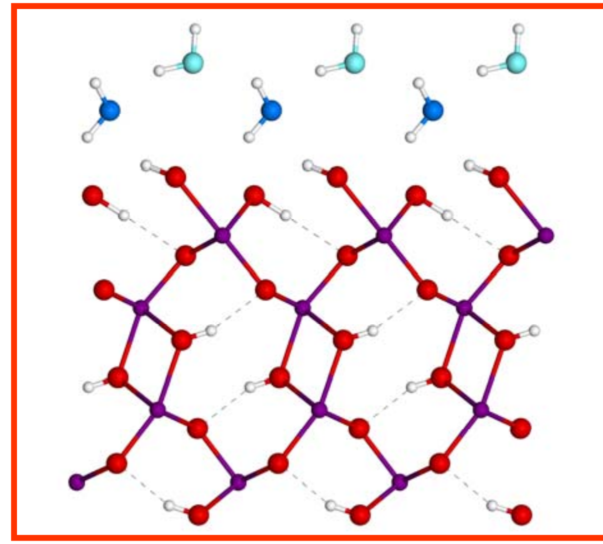

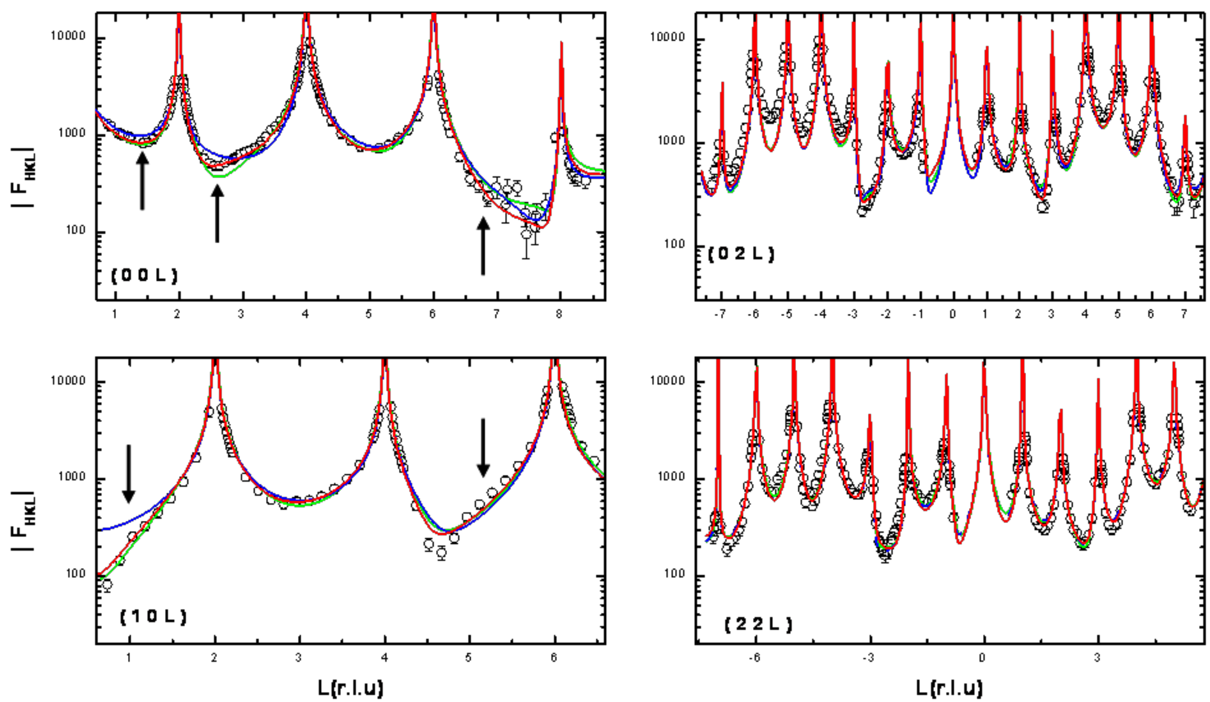

# Powder Diffraction - Real Time Reaction Studies: Fisher et al.

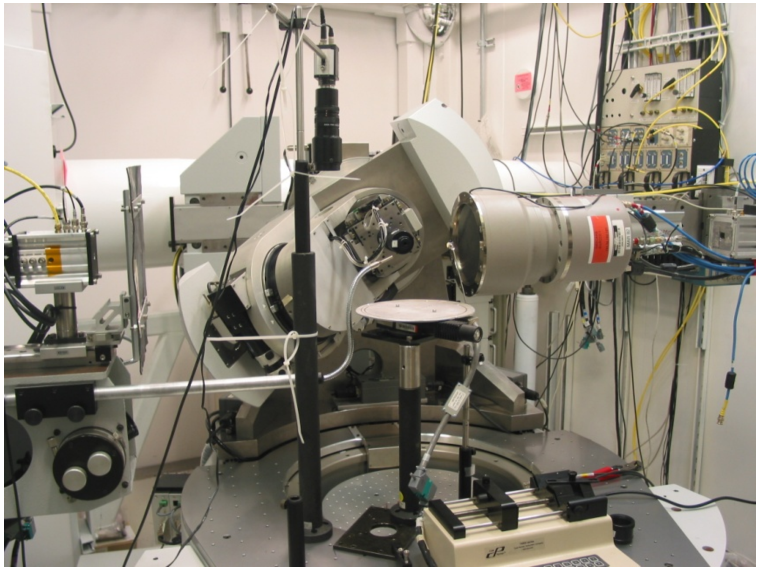

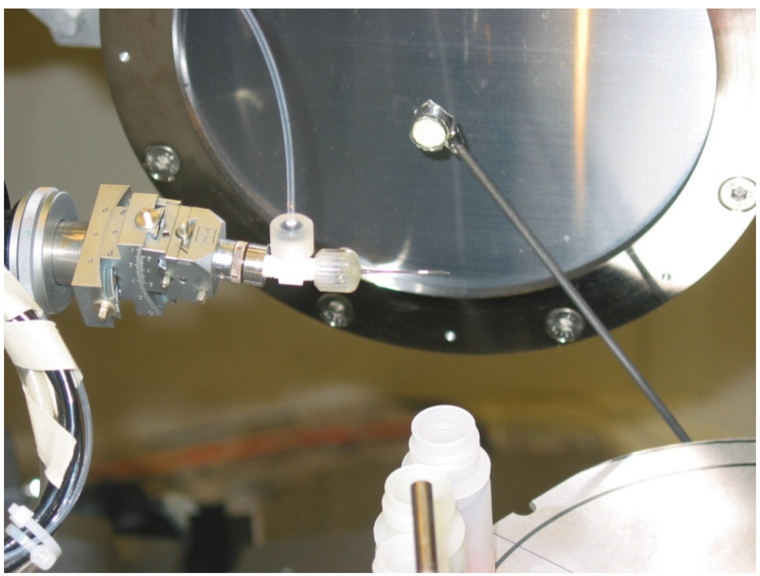

# X-ray Fluorescence Computed Tomography Using Emission Tomography Systems

L. J. Meng[1], P. J. La Riviere[2] and G. Fu[1], Peter Eng[3] and Matt Newville[3]
1. Department of Nuclear Plasma and Radiological Engineering, University of Illinois at Urbana-Champaign
2. Department of Radiology, University of Chicago
3. Consortium for Advanced Radiation Sources, University of Chicago

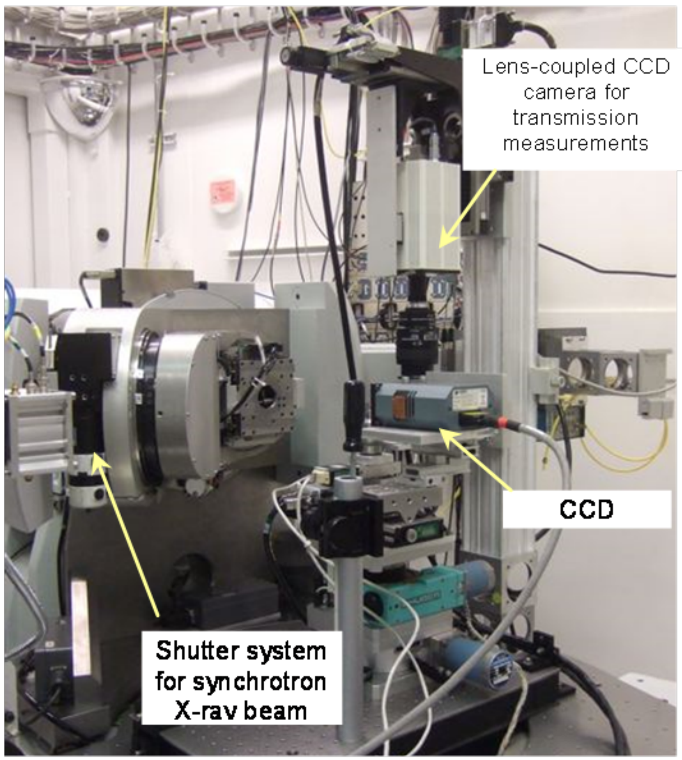


(a) Experimental Setup at Argonne APS beam line.

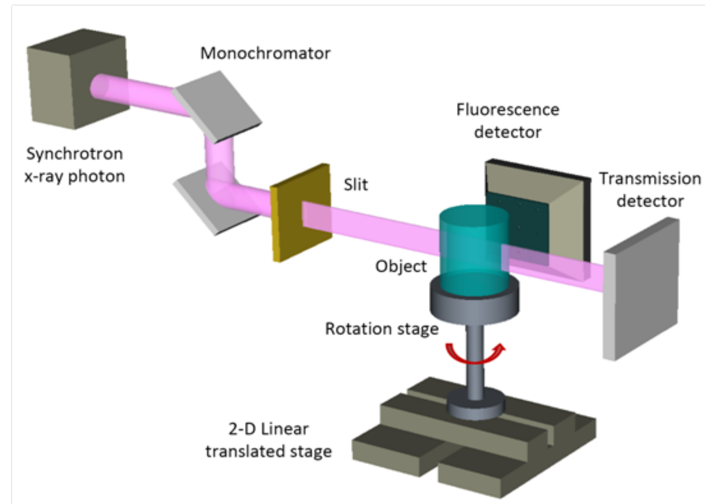


**(b)** Schematic of the experimental setup.

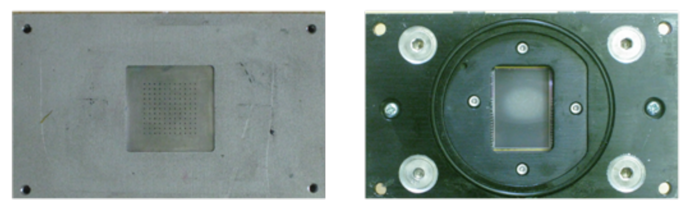

**(c)** The direct conversion X-ray CCD detector (right) and the collimation apertures used in this study (left). The aperture has 121 pinholes of 100μm diameter.

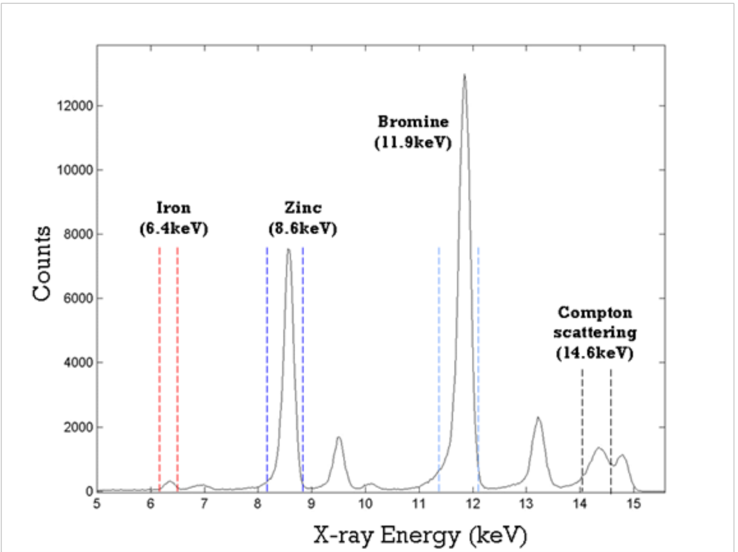


Fig. 5. Energy spectrum measured with the X-ray CCD detector. The energy threshold used for selecting fluorescence components are shown in the figure.

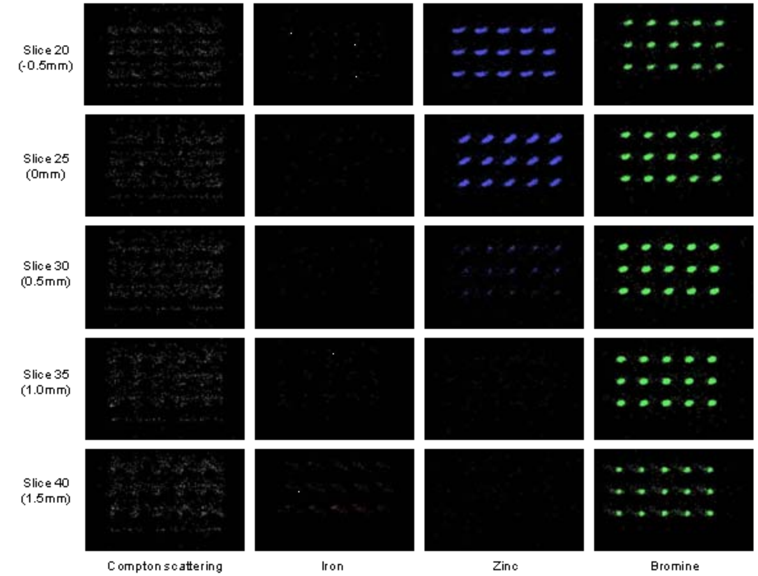


Fig. 6. Experimentally acquired projections with fluorescence and Compton scattered X-rays. The aperture used has 35 pinholes of 300μm diameter. The projection data was acquired by stepping a thin X-ray beam of 50μm thickness through the object. Data acquisition time was 5 minutes per slice.

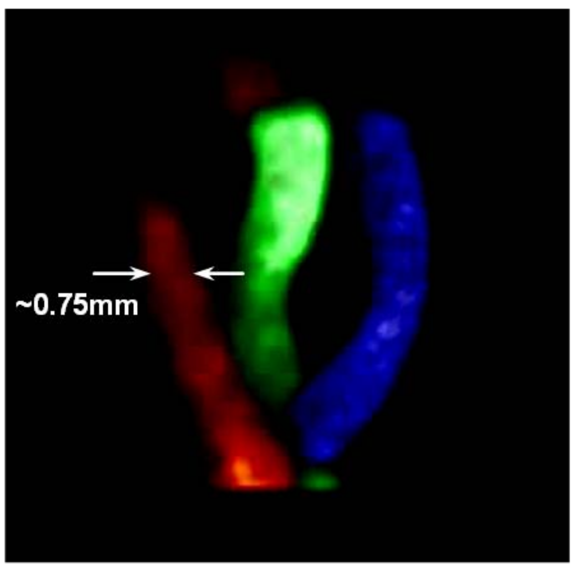


Fig. 7. 3-D rendering of the reconstructed elemental distribution with data acquired in Mode 2 geometry.

# 13-BM-D

- Source:
  - Accepts up to 2.5 mrad
  - Energy Range 5.6 – 70 keV (scannable, white and pink)
  - Focused to ~ 10 microns
  - Wide Beam 50 x 9 mm
- Experiments:
  1. High-pressure studies (DAC and LVP)
  2. Microcrystal Diffraction
  3. Microtomography / Radiography (Mono and Pink)
  4. Spectroscopy (EXAFS)
  5. XRF Microprobe

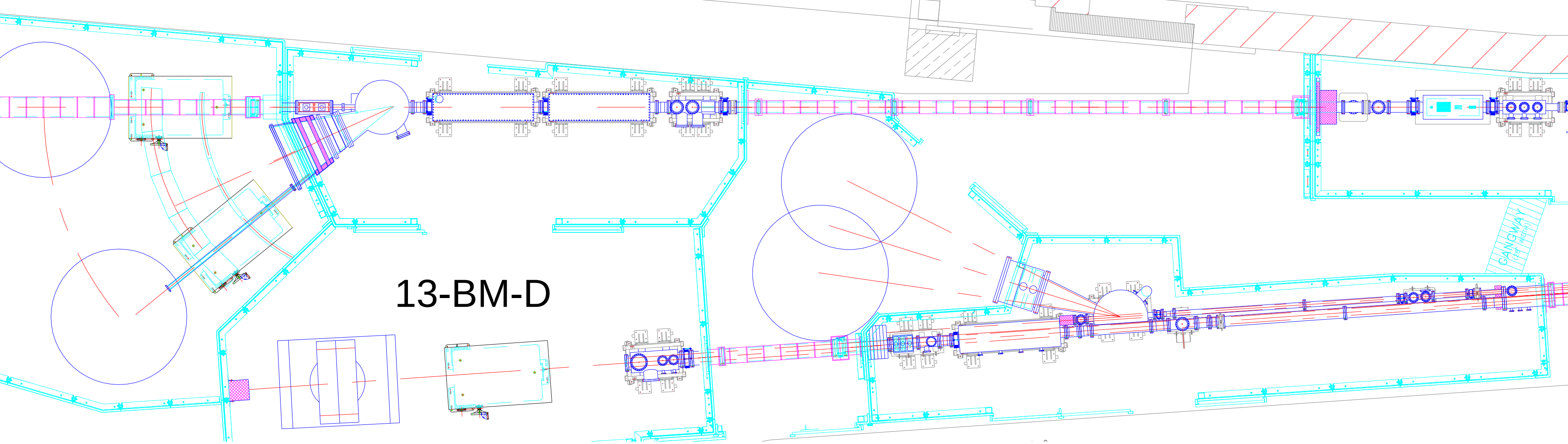
13-BM-D
GANGWAY


13-BM-D
GeoSoilEnviroCARS
DANGER

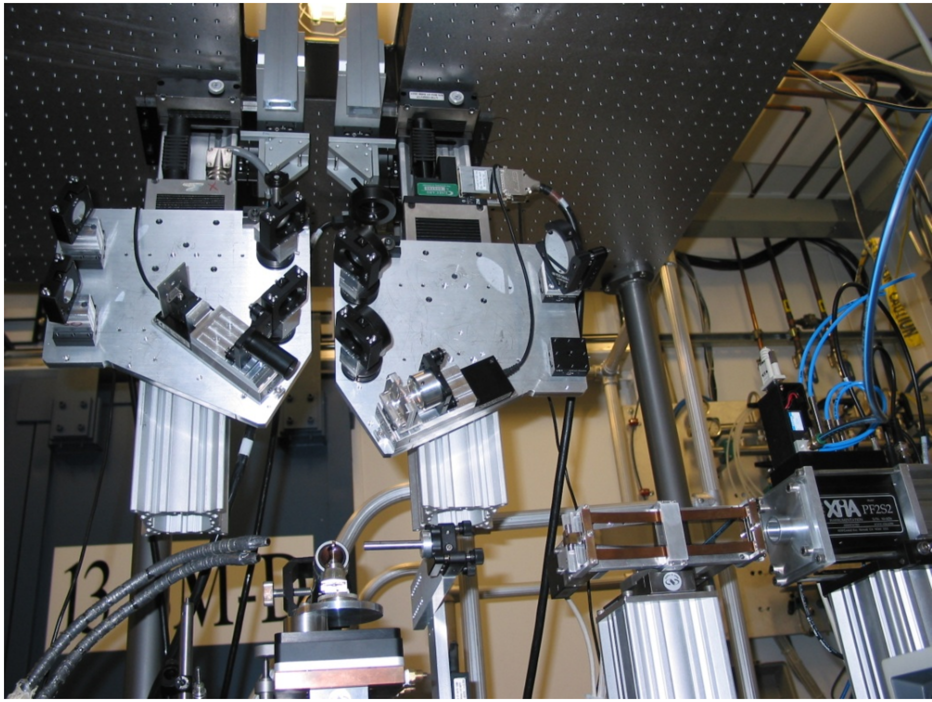

# 13-BM-D DAC

***The full spectroscopic characterization of a sample is possible in-situ at extreme high pressure/temperature conditions with powerful combination of x-ray diffraction, Brillouin, Raman and fluorescence spectroscopy applied to a single point on the sample in a diamond anvil cell***

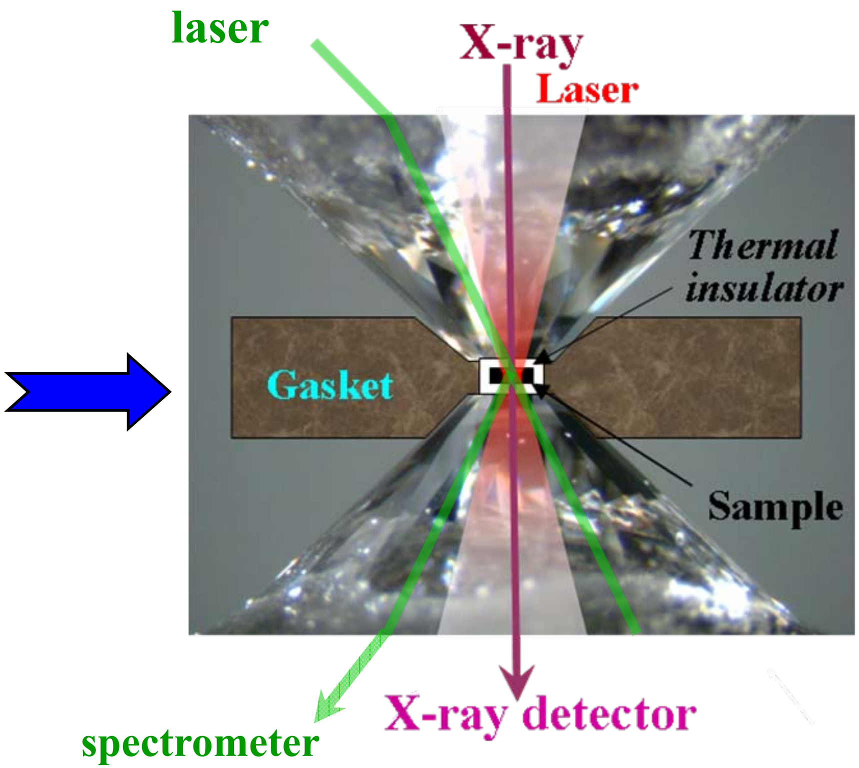

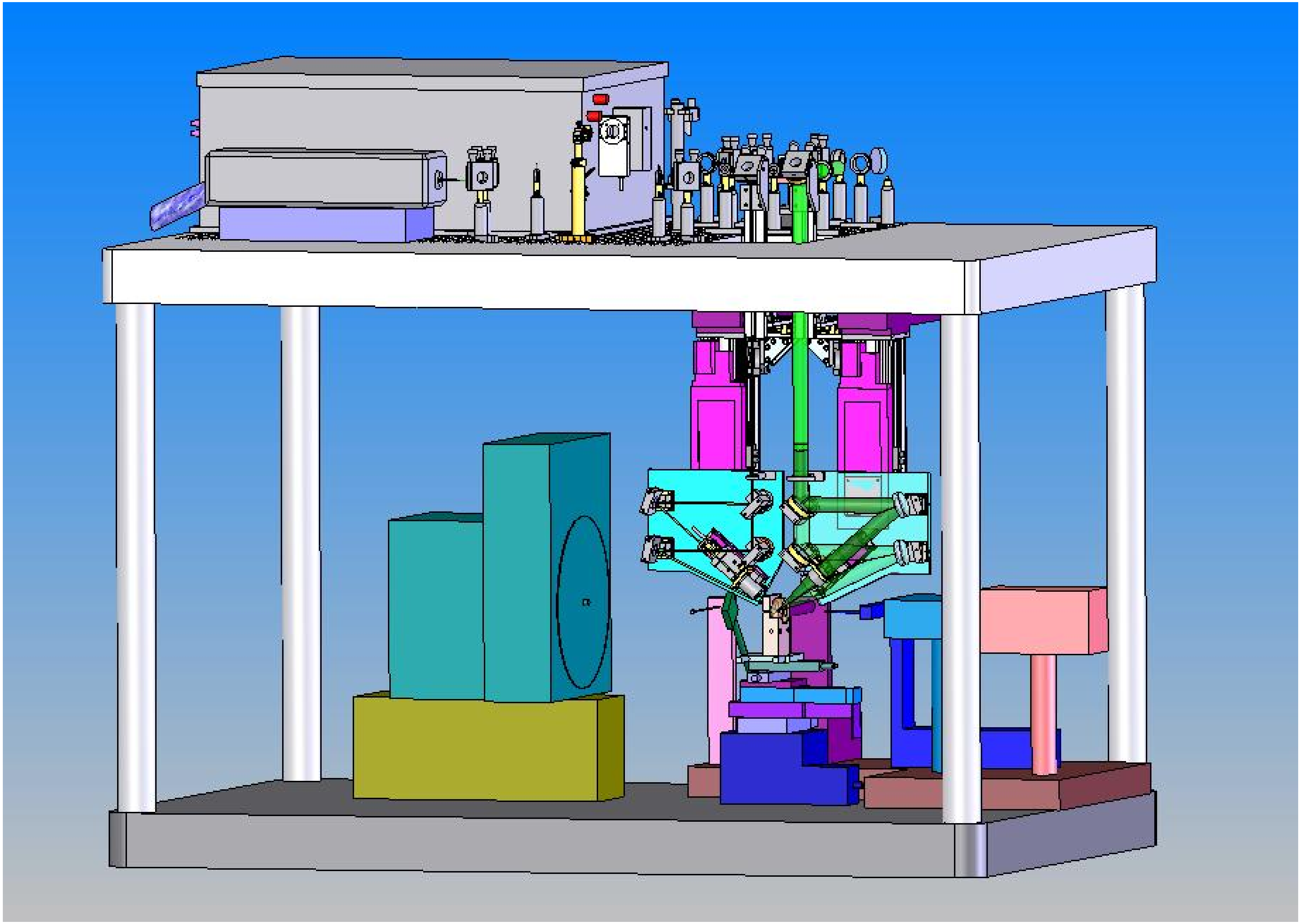

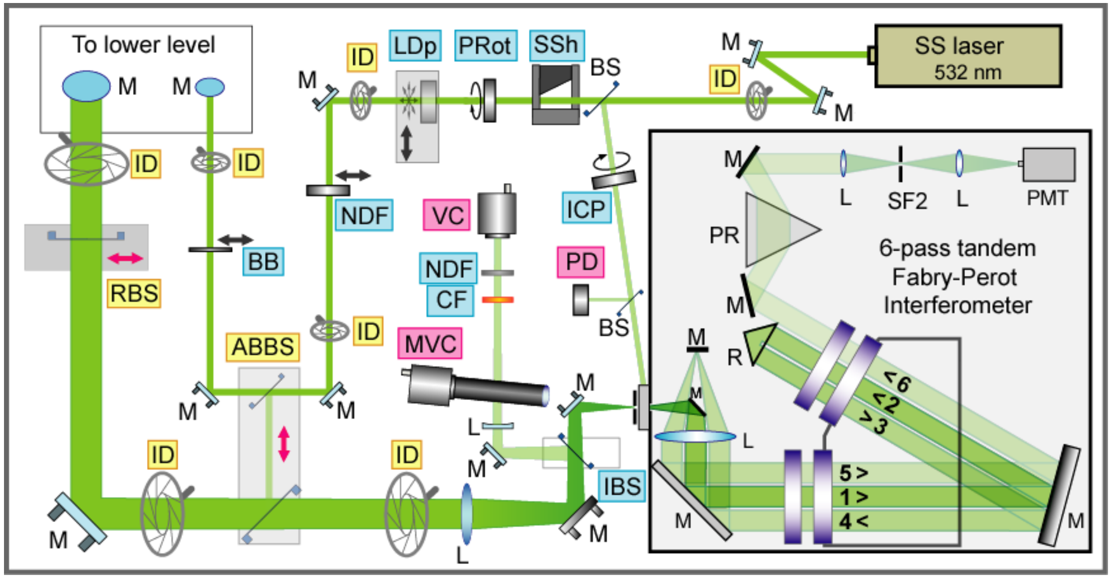

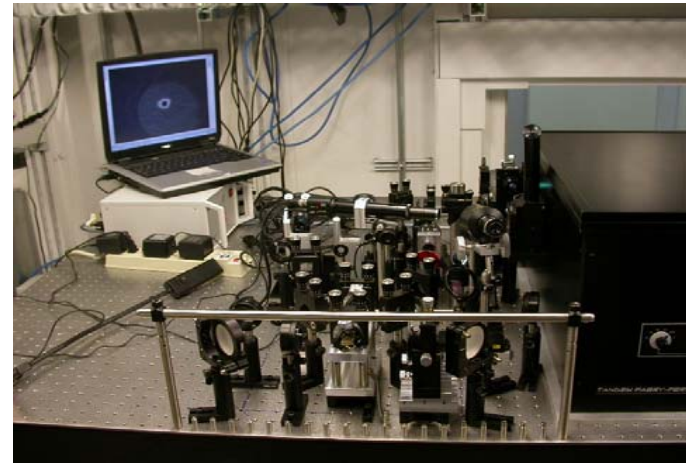
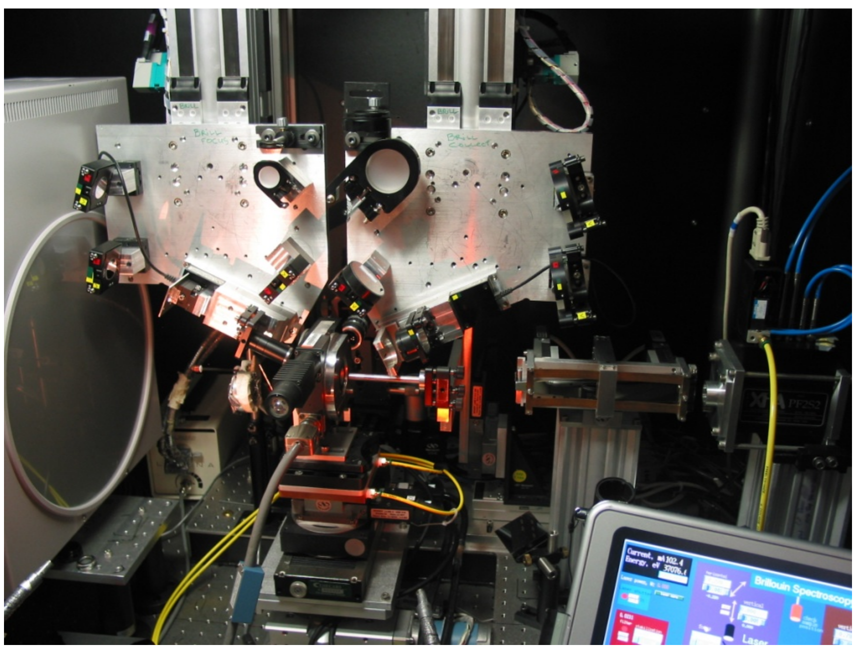
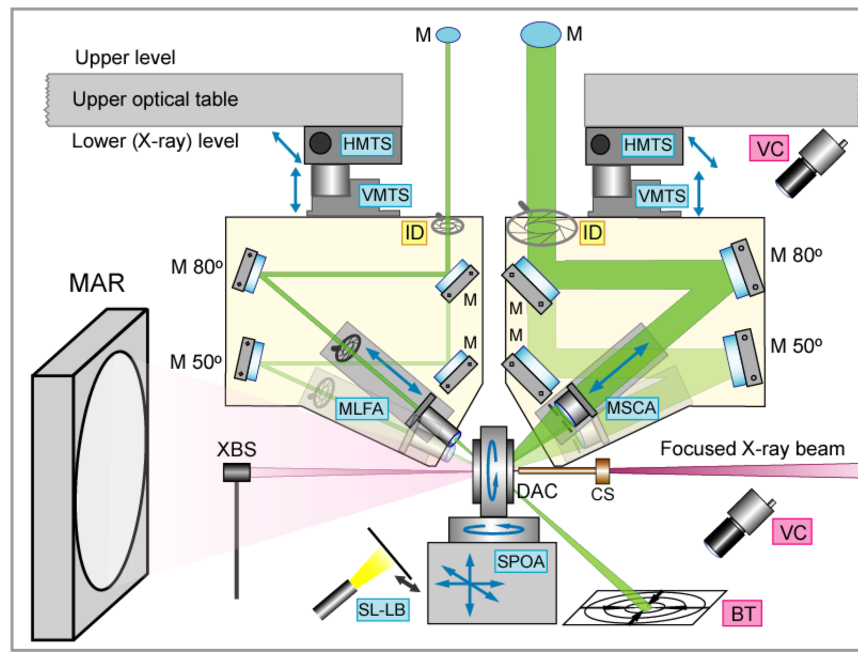


S. V. Sinogeikin, J. D. Bass, V.B. Prakapenka, Rev. Sci. Instrum. 77, 103905 2006

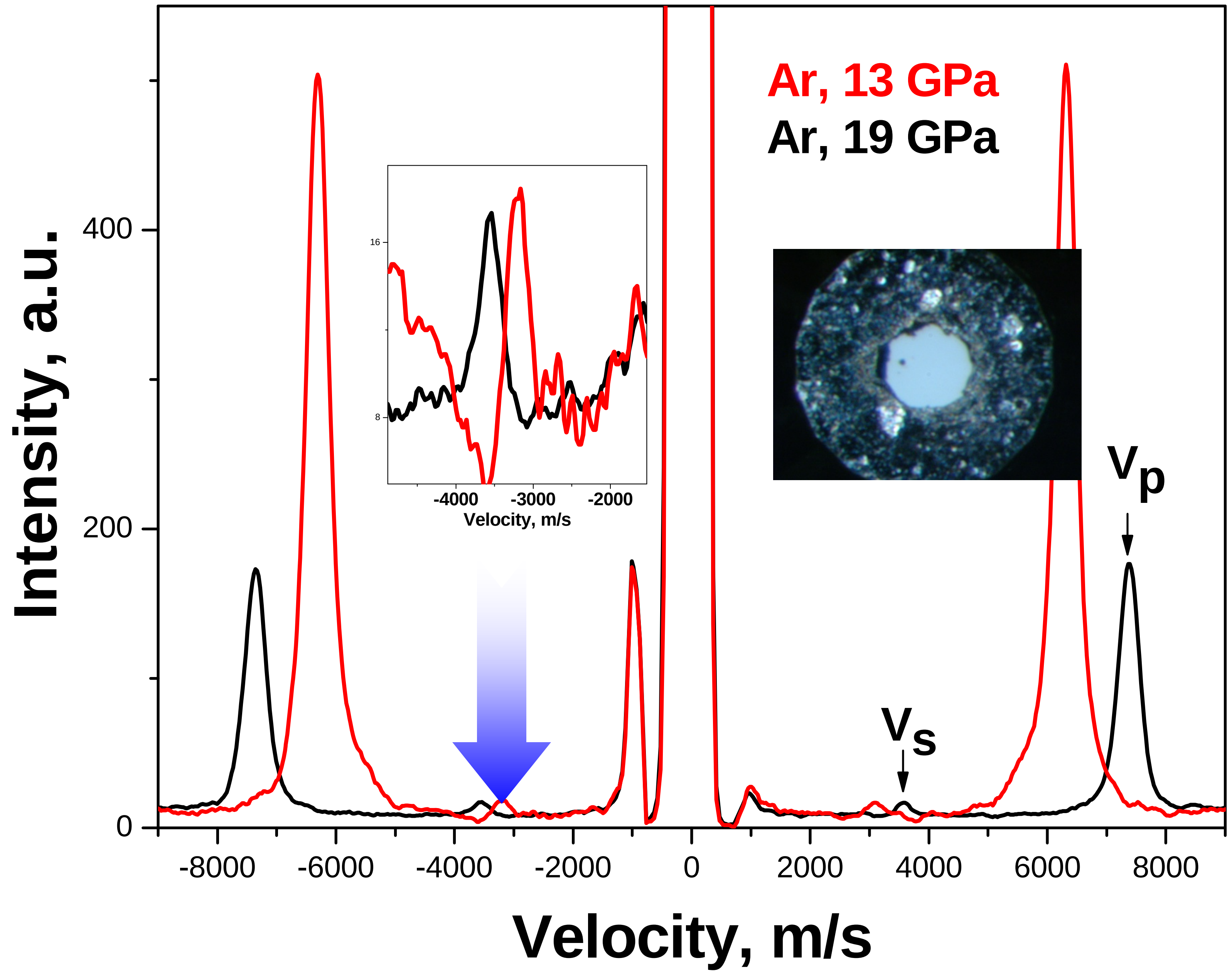

Ar, 13 GPa
Ar, 19 GPa
Intensity, a.u.
Velocity, m/s
V_p
V_s
0
200
400
-8000
-6000
-4000
-2000
0
2000
4000
6000
8000
16
8
-4000
-3000
-2000
Velocity, m/s

# XRD and BS of single crystal MgO in [100] direction in the DAC at 4 GPa

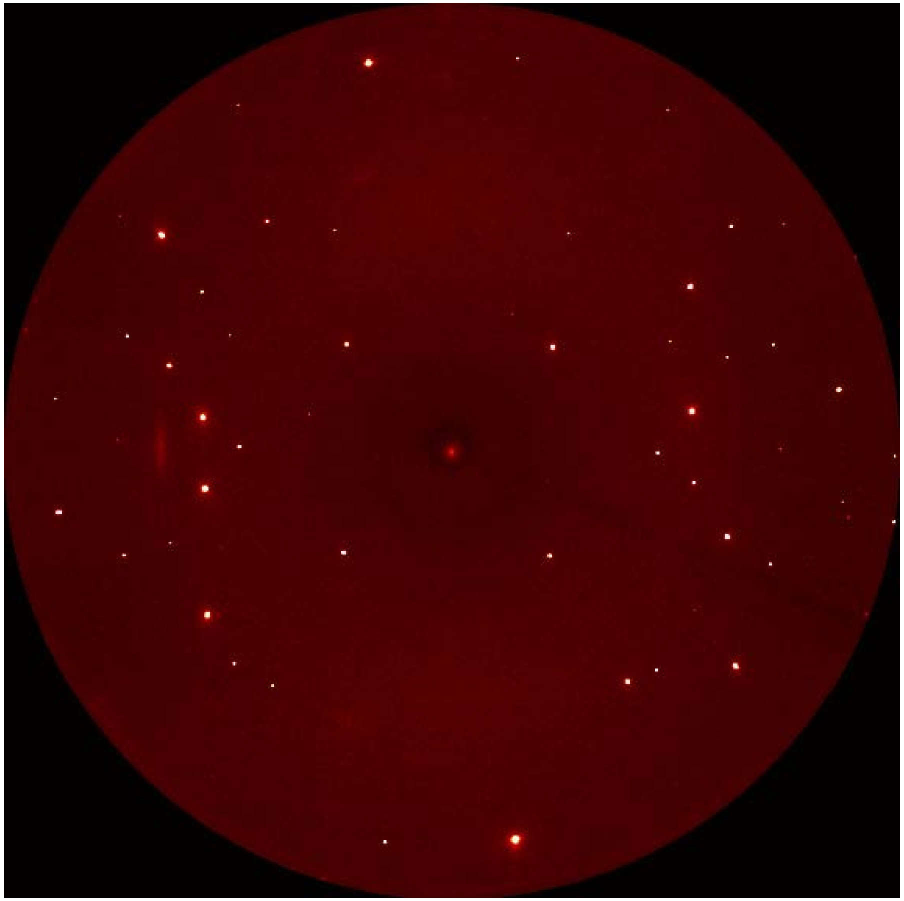

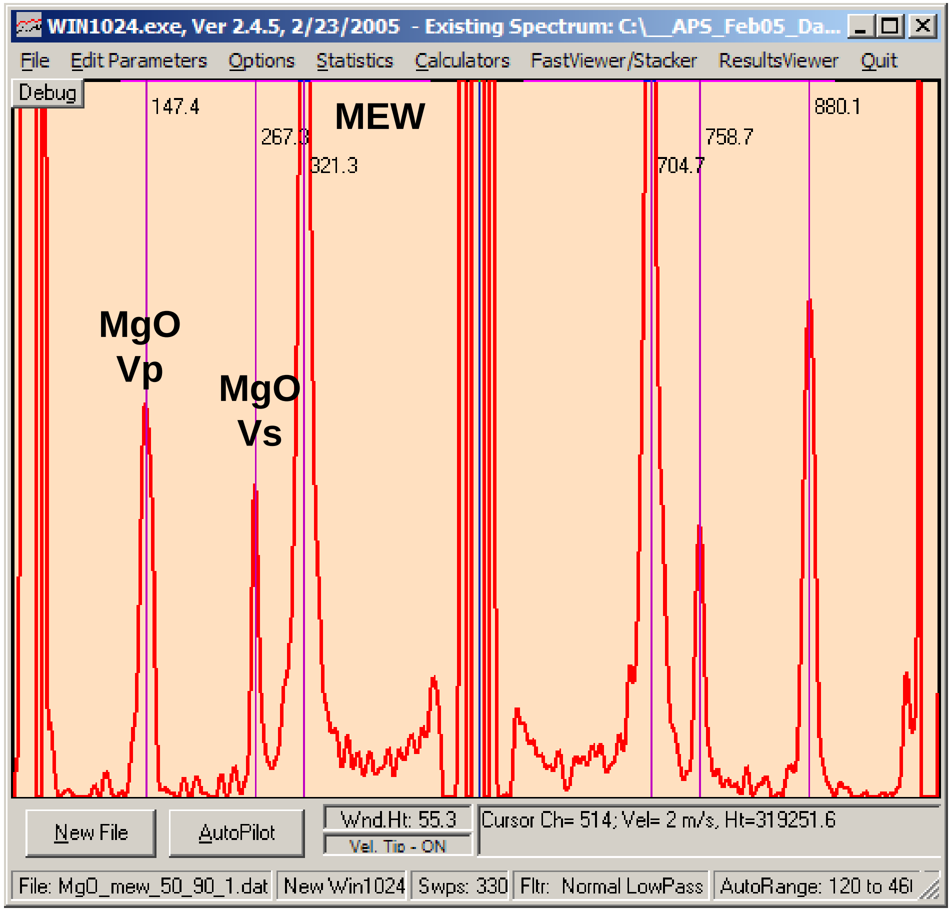


S. V. Sinogeikin, J. D. Bass, V.B. Prakapenka, Rev. Sci. Instrum. 77, 103905 2006

# Monitor the thermal decomposition of lizardite (a serpentine mineral) up to 1000 K.

Mark Frank

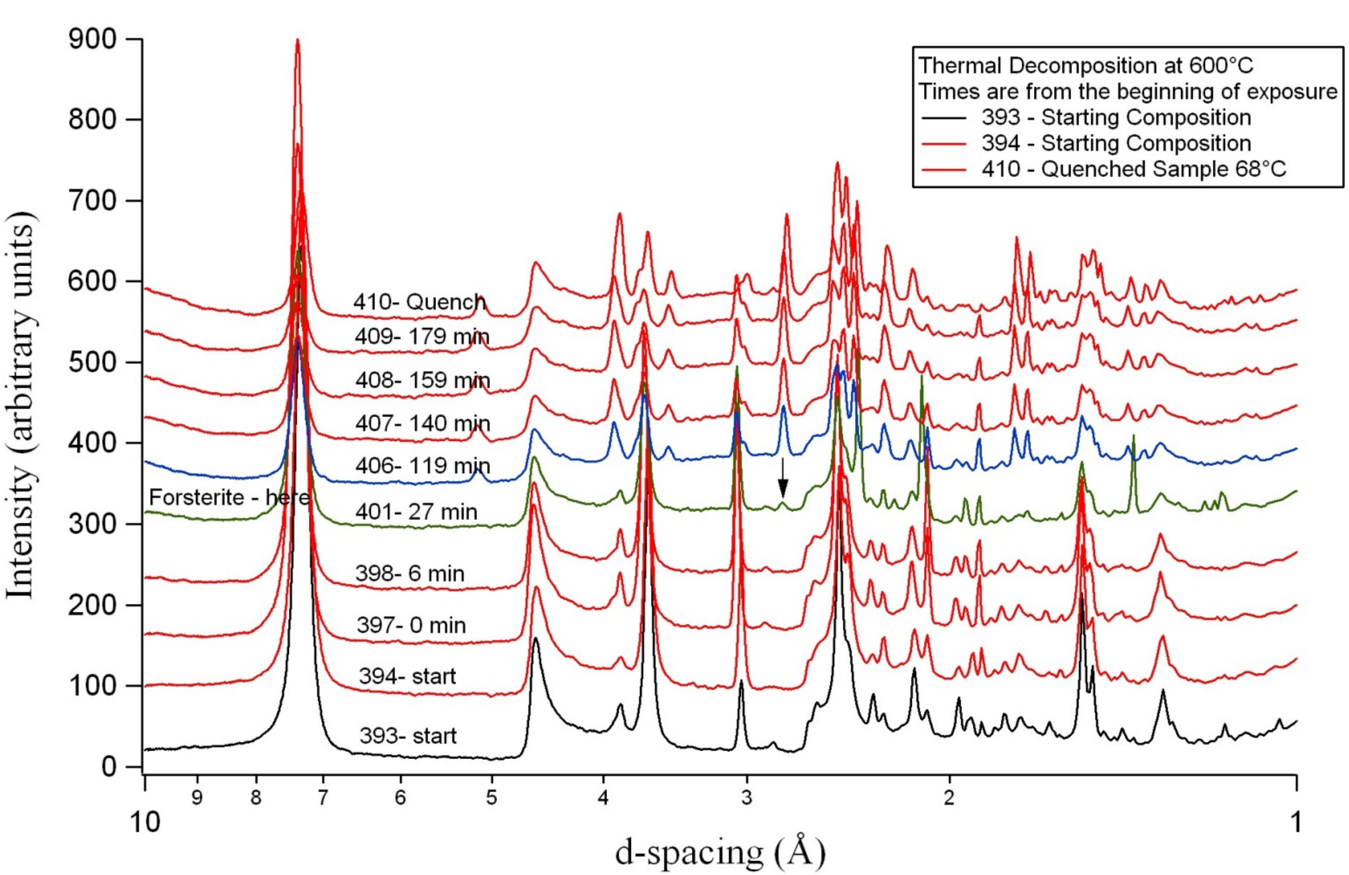


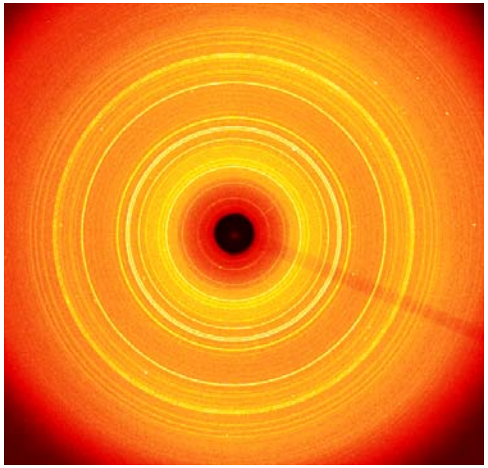

*Angle Dispersive X-ray diffraction pattern taken of reaction products (700°C) with online imaging system (MAR345)*

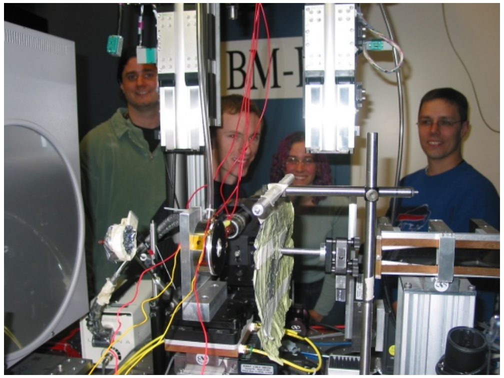


**Potential reaction at 550-600°C.**

$Mg_6Si_4O_{10}(OH)_8 \rightarrow 3\ Mg_2SiO_4 + 4\ H_2O + SiO_2$

**Lizardite** **Forsterite** **amorphous**

# 13-BM-D LVP

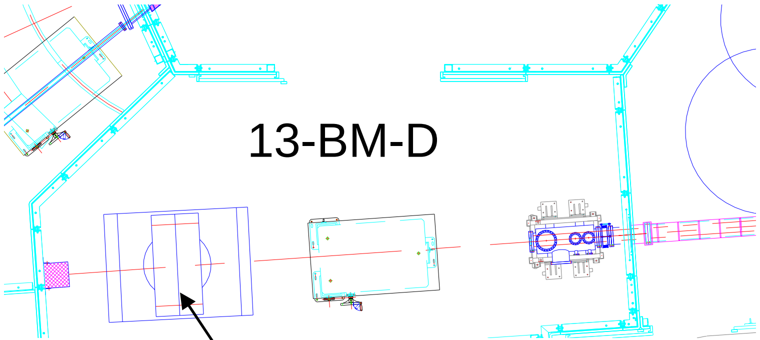


250 T LVP

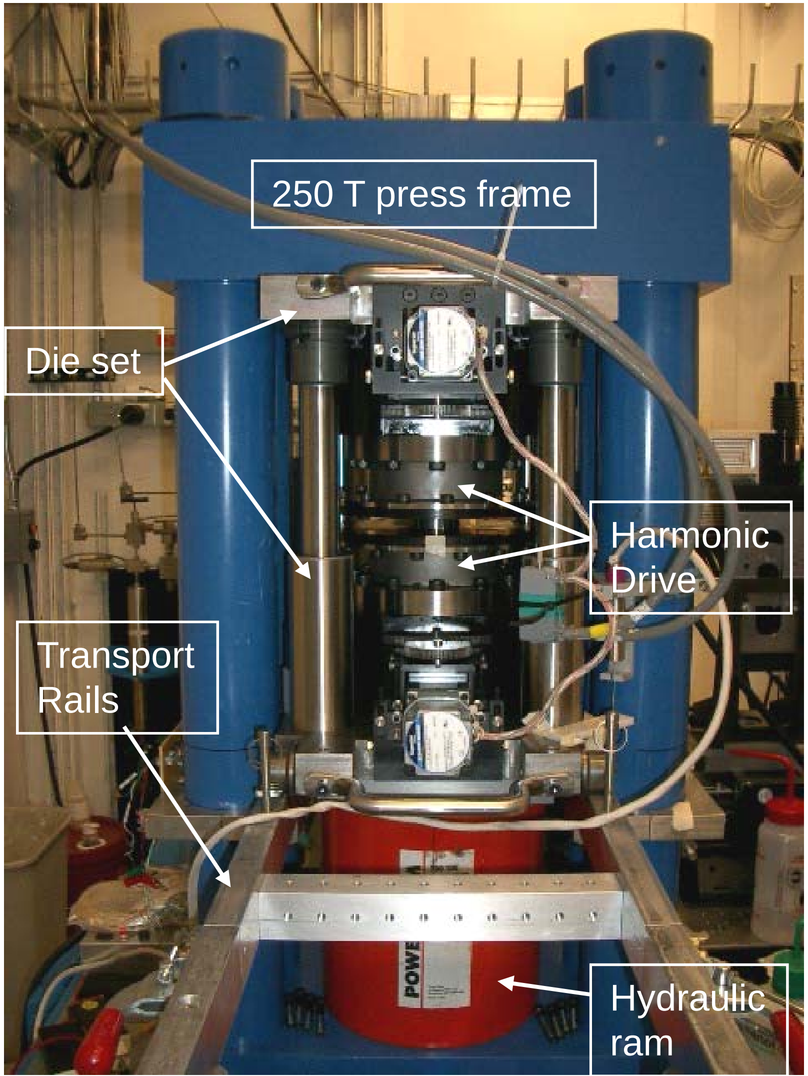

# *Rheology at high P-T*

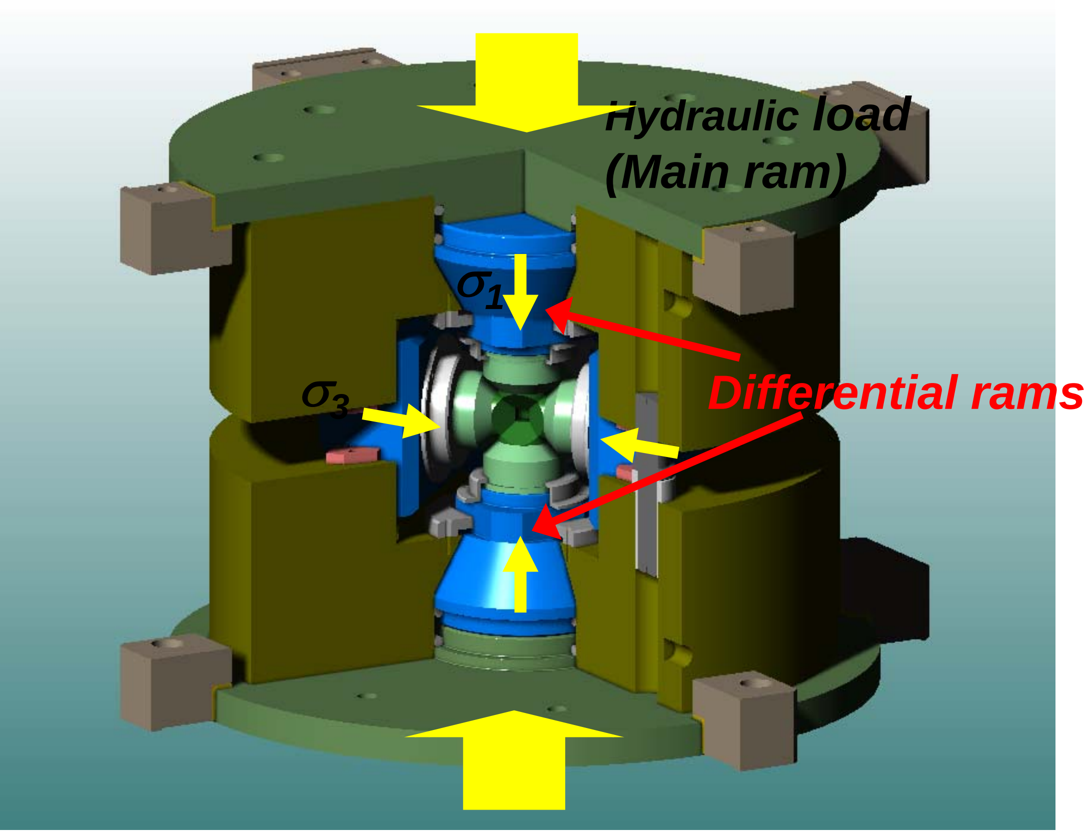


D-DIA (Wang et al., 2003)

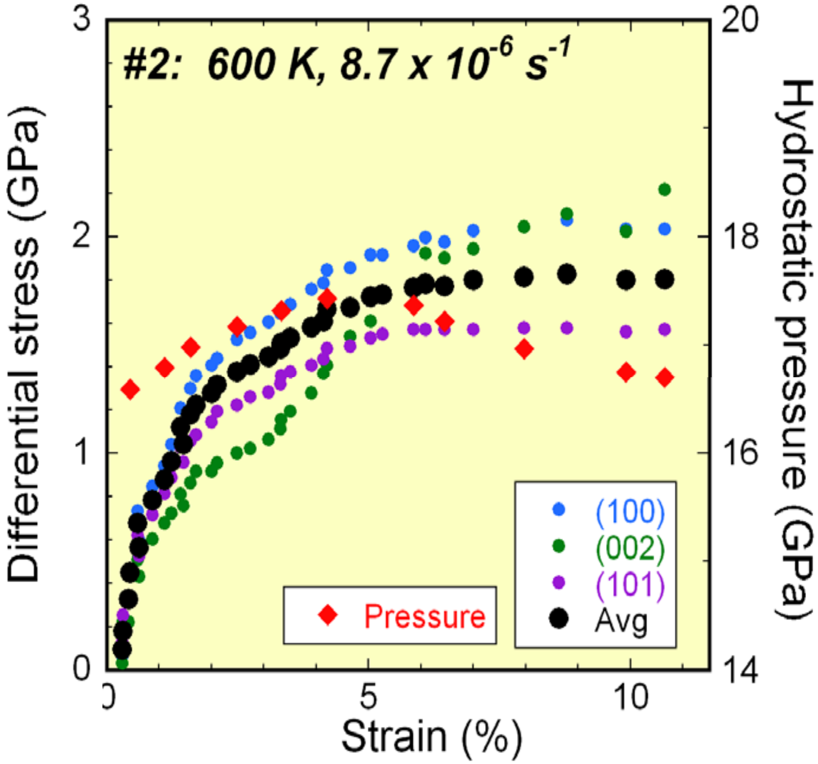


Deformation of hcp-Fe to 18 GPa, 700 K

# High pressure tomography

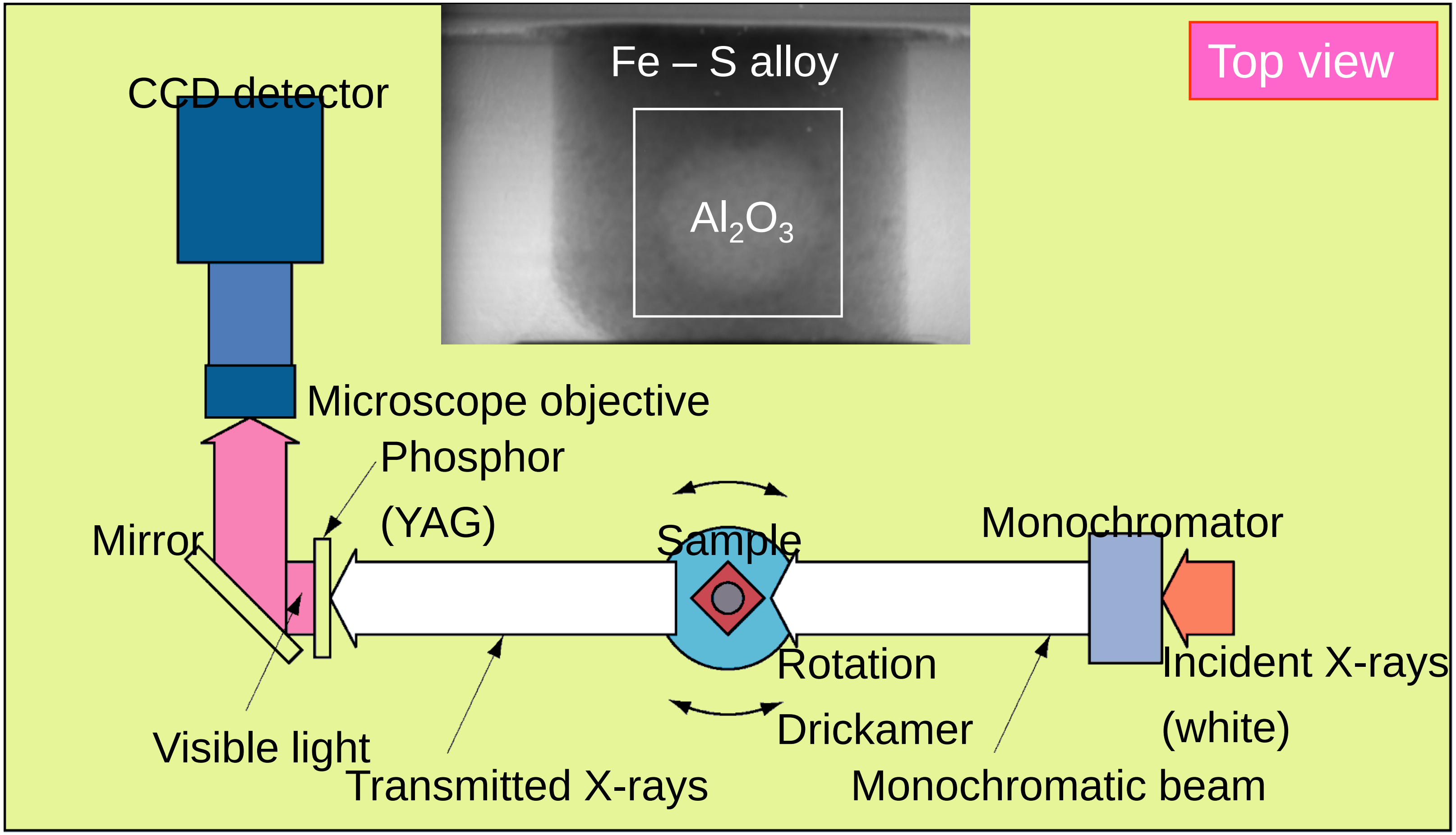

# High-P tomography

## Goal: Measure volumes of melts at high pressure

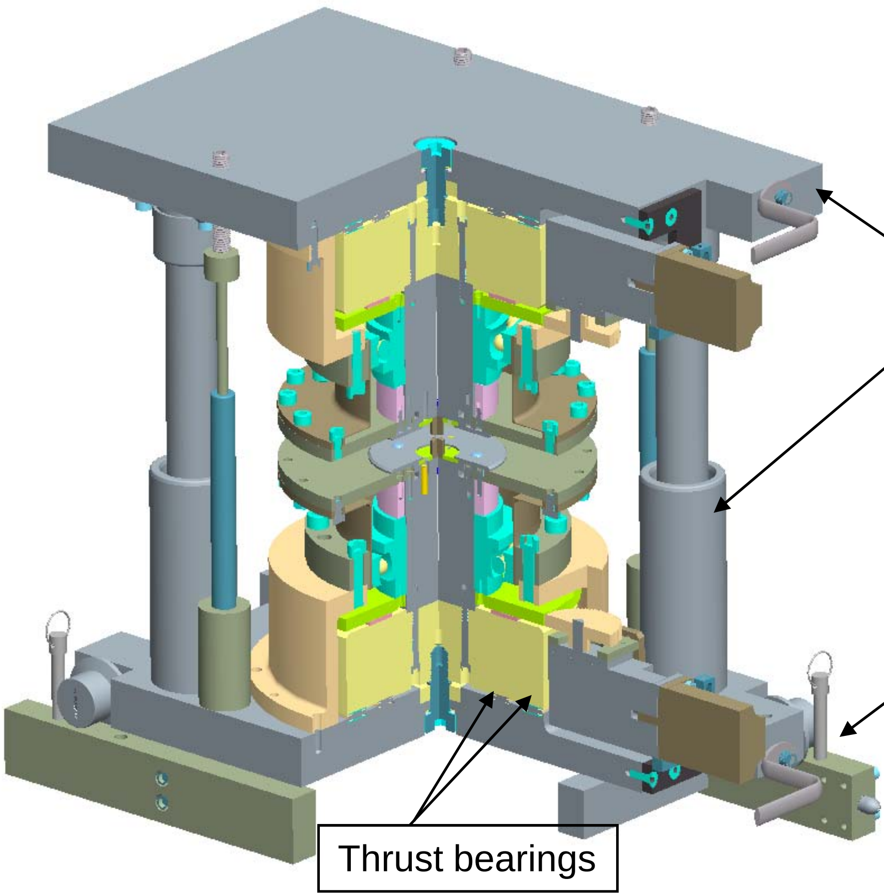


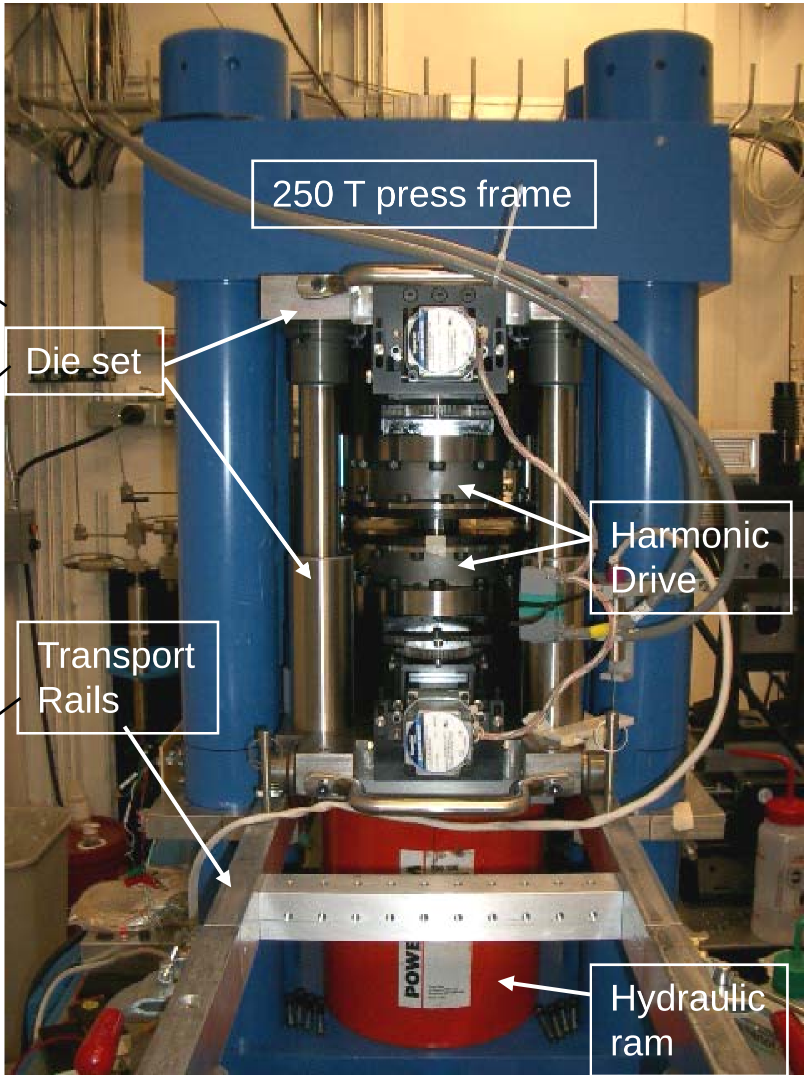

*High-P microtomography: 3D imaging of texture at P, T and strains*

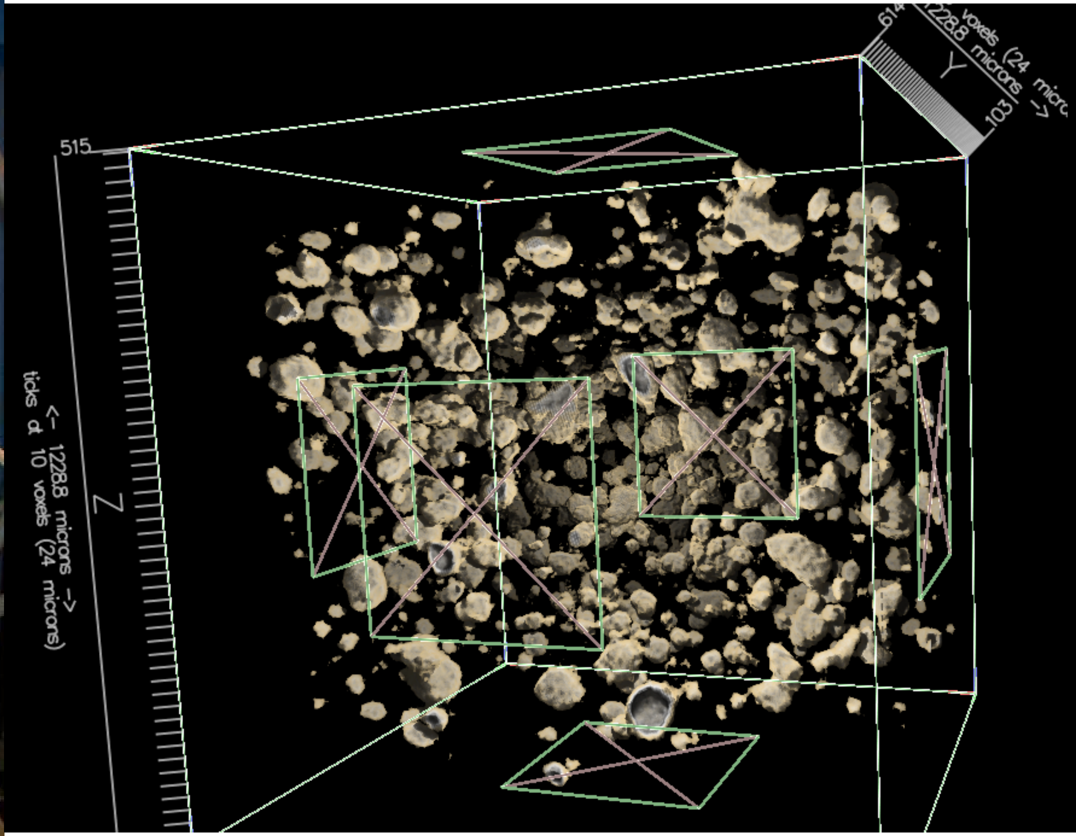

# *Viscosity of Melts Under High P-T*

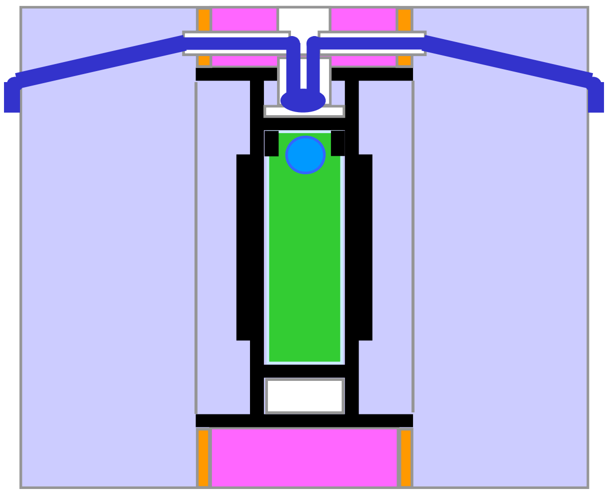

$$\sigma = \eta \dot{\varepsilon}$$

Terminal velocity:

$v_t = (2\,\Delta\rho\, r^2\, g) / (9\,\eta)$

$\Delta\rho = \rho_{sphere} - \rho_{melt}$

$r$ = sphere radius.

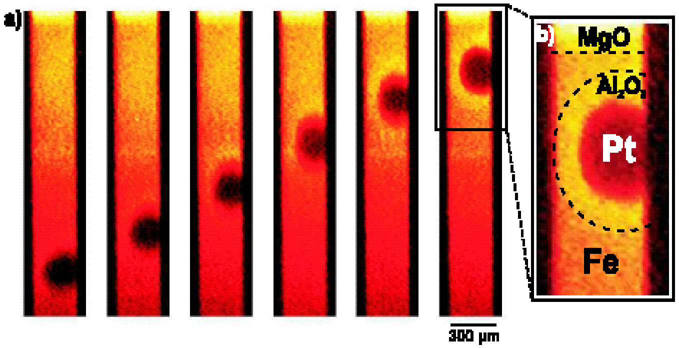


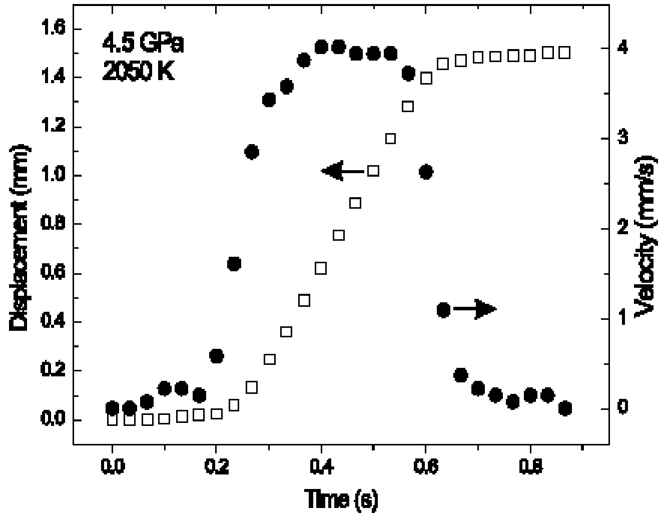


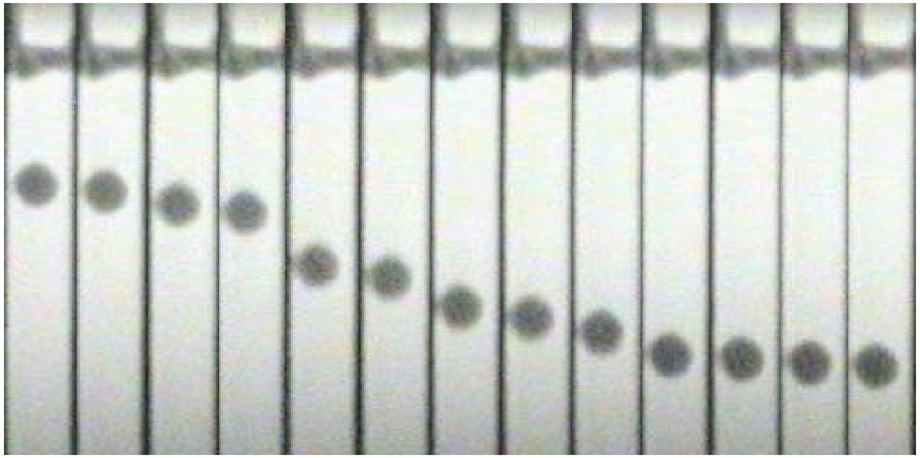

Diopside, 5 GPa, 2100 K

Pure Fe at 2050 K (Rutter et al., PRB’02)

# Absorption Tomography Setup
## 13-BM-D station at APS

- X-ray Source
  - Parallel monochromatic x-rays, 8-65 keV
  - APS bending magnet source, 20 keV critical energy
  - 1-50mm field of view in horizontal, up to 6 mm in vertical
- Imaging System
  - YAG single crystal scintillator
  - 5X to 20X microscope objectives, or zoom/macro lens
  - 1Kx1Kpixel CCD camera
- Data collection
  - Rotate sample 180 degrees, acquire images every 0.25 degrees
  - Data collection time: 10 minutes
  - Reconstruction time: 5 minutes

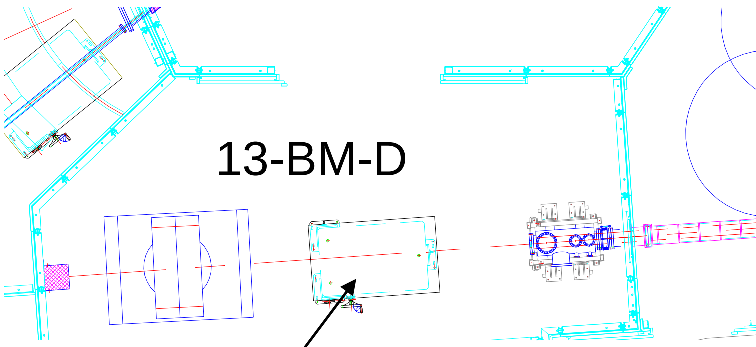


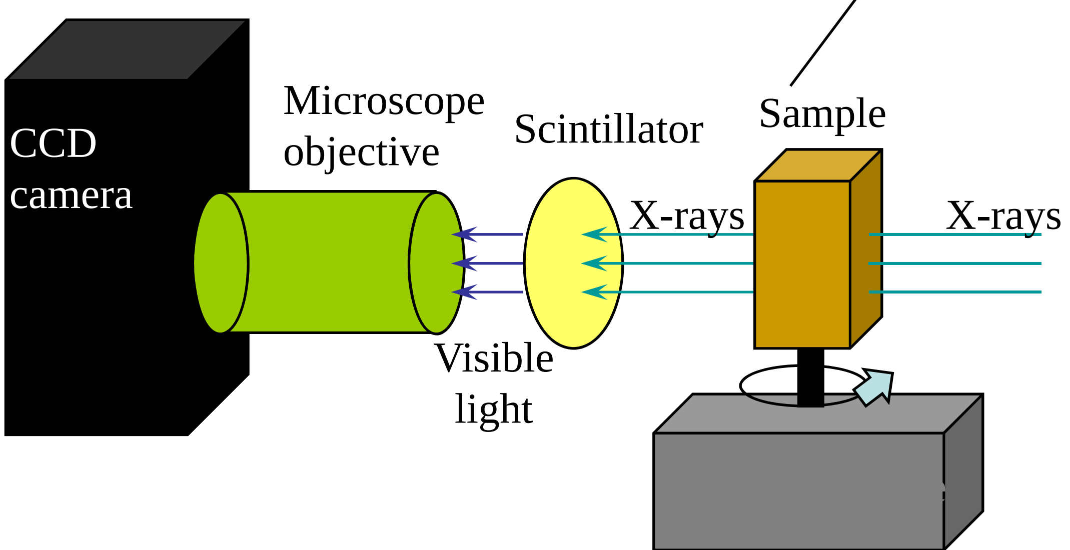

# Differential Absorption Tomography

Clint Willson (Louisiana State University)

8mm diameter sand column with aqueous phase containing Cs and organic phase containing I.

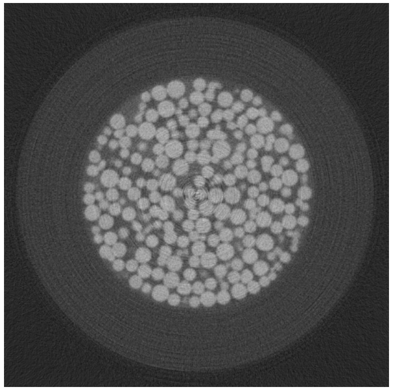

32.5 keV, below I and Cs K absorption edges

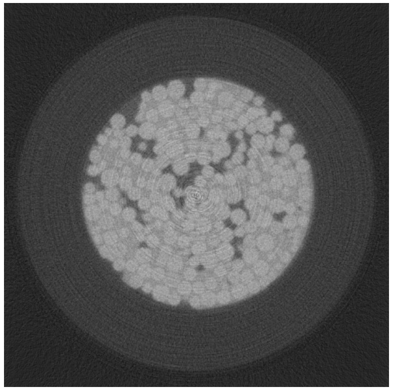

33.2 keV, above I and below Cs K absorption edges

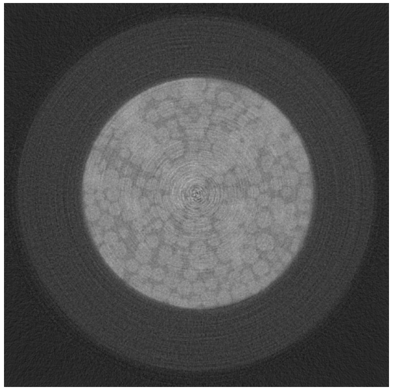

36.0 keV, above I and Cs K absorption edges

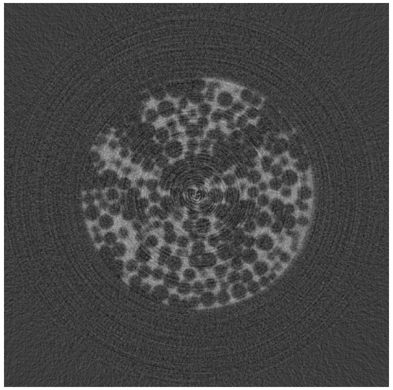

33.2 - 32.5 keV, showing distribution of I in the organic phase

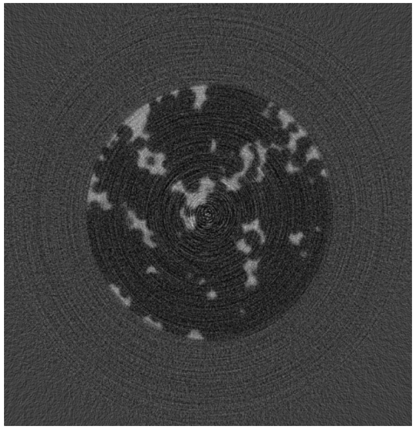

36.0 - 33.2, showing distribution of Cs in the aqueous phase

# High-Speed Radiography of Granular Particle Jets

**John Royer, University of Chicago Physics Dept.**

Sphere falling into a granular particle (e.g. sand) bed produces a jet

These images are above the surface, done with visible light

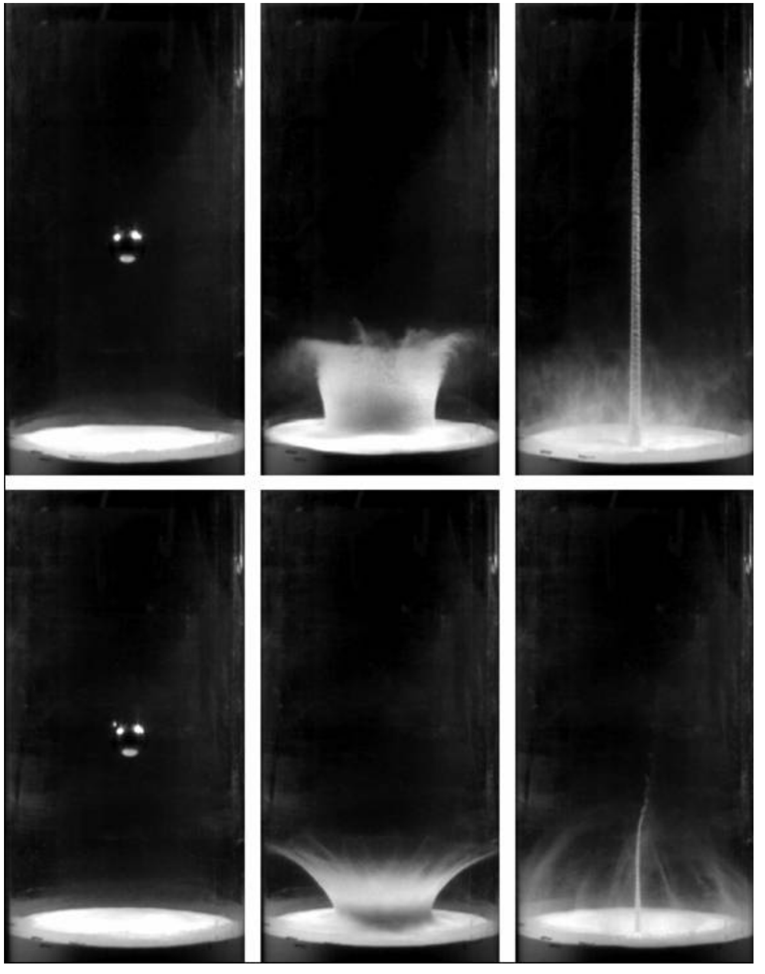

1 atmosphere

Reduced pressure

Want to understand what is happening below the surface

Used “pink” x-ray beam, high speed radiography

100 μsec exposure time, 5000 frames/sec

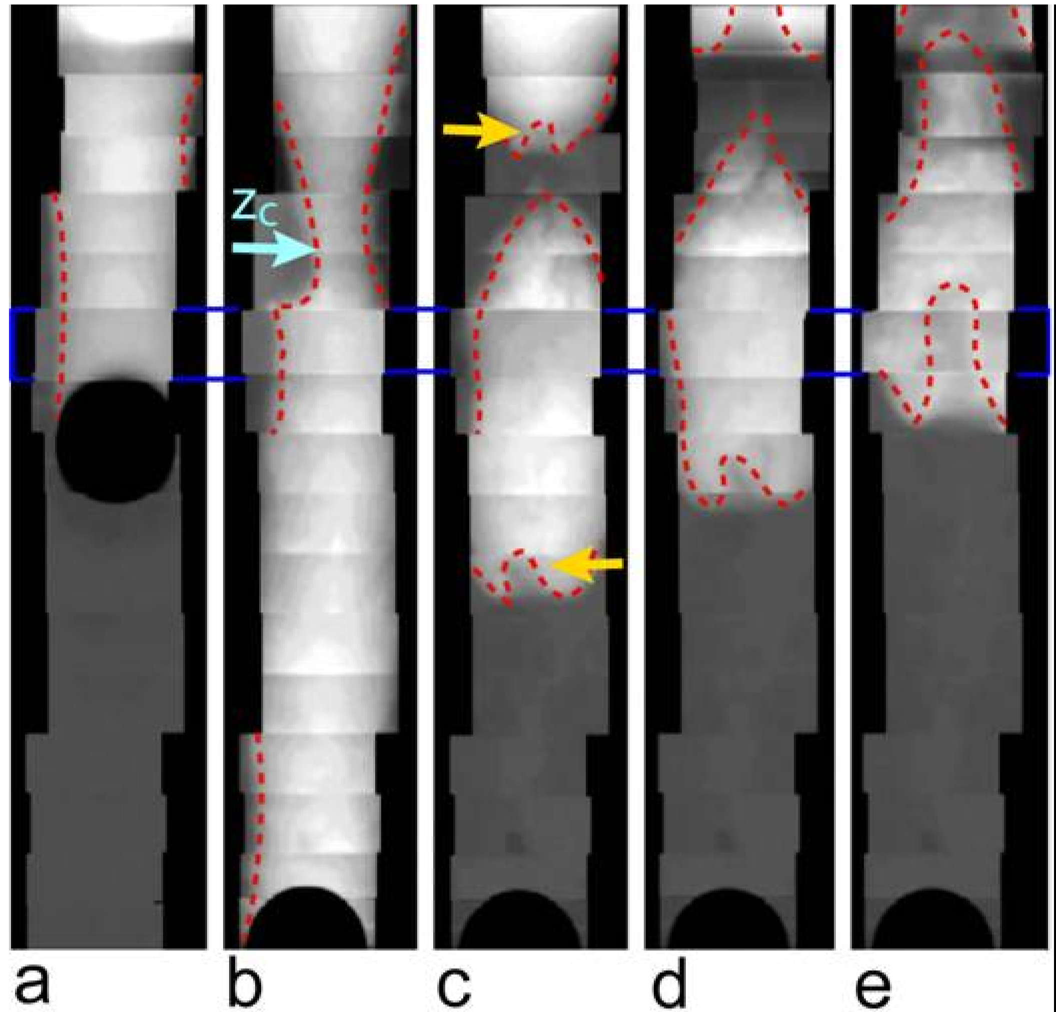

## January

| Date | ESAF | Tech | 00:00 - 08:00 | 08:00 - 16:00 | 16:00 - 24:00 |
|---|---|---|---|---|---|
| 1 | | | | | |
| 2 | | | | | |
| 3 | | | | | |
| 4 | | | | | |
| 5 | | | | | |
| 6 | | | | | |
| 7 | | | | | |
| 8 | | | | | |
| 9 | | | | | |
| 10 | | | | | |
| 11 | | | | | |
| 12 | | | | | |
| 13 | | | | | |
| 14 | | | | | |
| 15 | | | | | |
| 16 | | | | | |
| 17 | | | | | |
| 18 | | | | | |
| 19 | | | | | |
| 20 | | | | | |
| 21 | | | | | |
| 22 | | | | | |
| 23 | | | | | |
| 24 | | | | | |
| 25 | | | | | |
| 26 | | | | | |
| 27 | | | | | |
| 28 | 1 | DAC | | DAC Setup | DAC Setup |
| 29 | 2 | | DAC Setup | A. Goncharov GUP 10524 | A. Goncharov GUP 10524 |
| 30 | | | A. Goncharov GUP 10524 | A. Goncharov GUP 10524 | A. Goncharov GUP 10524 |
| 31 | | | A. Goncharov GUP 10524 | A. Goncharov GUP 10524 | A. Goncharov GUP 10524 |

## February

| Date | ESAF | Tech | 00:00 - 08:00 | 08:00 - 16:00 | 16:00 - 24:00 |
|---|---|---|---|---|---|
| 1 | 3 | | A. Goncharov GUP 10524 | I. Kantor GUP 11274 | I. Kantor GUP 11274 |
| 2 | | | I. Kantor GUP 11274 | I. Kantor GUP 11274 | I. Kantor GUP 11274 |
| 3 | | | I. Kantor GUP 11274 | | |
| 4 | | | | I. Kantor GUP 11274 | I. Kantor GUP 11274 |
| 5 | 4 | | I. Kantor GUP 11274 | Marquardt GUP 1173 | Marquardt GUP 1173 |
| 6 | | | Marquardt GUP 1173 | Marquardt GUP 1173 | Marquardt GUP 1173 |
| 7 | | | Marquardt GUP 1173 | Marquardt GUP 1173 | Marquardt GUP 1173 |
| 8 | 5 | | Marquardt GUP 1173 | Tait GUP 11472 | Tait GUP 11472 |
| 9 | | | Tait GUP 11472 | | |
| 10 | | | | | |
| 11 | | | | Tait GUP 11472 | Tait GUP 11472 |
| 12 | 6 | | Tait GUP 11472 | Horita GUP 11083 | Horita GUP 11083 |
| 13 | | | Horita GUP 11083 | Horita GUP 11083 | Horita GUP 11083 |
| 14 | 7 | CMT | Horita GUP 11083 | CMT Setup | CMT Setup |
| 15 | 8 | | CMT Setup | Costanza-Robinson GUP 10019 | Costanza-Robinson GUP 10019 |
| 16 | 9 | | Costanza-Robinson GUP 10019 | Tick GUP 11385 | Tick GUP 11385 |
| 17 | | | Tick GUP 11385 | | |
| 18 | 10 | | | Brusseau GUP 11132 | Brusseau GUP 11132 |
| 19 | | | Brusseau GUP 11132 | Brusseau GUP 11132 | Brusseau GUP 11132 |
| 20 | 11 | | Brusseau GUP 11132 | Friedrich GUP 10968 | Friedrich GUP 10968 |
| 21 | 12 | | Friedrich GUP 10968 | Claiborne GUP 11396 | Claiborne GUP 11396 |
| 22 | 13 | | Claiborne GUP 11396 | Pamukcu GUP 11351 | Pamukcu GUP 11351 |
| 23 | | | Pamukcu GUP 11351 | | |
| 24 | | | | | |
| 25 | 14 | | | Kramer GUP 11148 | Kramer GUP 11148 |
| 26 | | | Kramer GUP 11148 | Kramer GUP 11148 | Kramer GUP 11148 |
| 27 | 15 | | Kramer GUP 11148 | Roeder GUP 10463 | Roeder GUP 10463 |
| 28 | 16 | | Roeder GUP 10463 | Pokroy GUP 11217 | Pokroy GUP 11217 |

## March

| Date | ESAF | Tech | 00:00 - 08:00 | 08:00 - 16:00 | 16:00 - 24:00 |
|---|---|---|---|---|---|
| 1 | 17 | | Pokroy GUP 11217 | Smucker GUP 9452 | Smucker GUP 9452 |
| 2 | | | Smucker GUP 9452 | Smucker GUP 9452 | Smucker GUP 9452 |
| 3 | | | Smucker GUP 9452 | | |
| 4 | 18 | LVP | | LVP HPXTM Setup | LVP HPXTM Setup |
| 5 | 19 | | LVP HPXTM Setup | Watson GUP 11198 | Watson GUP 11198 |
| 6 | | | Watson GUP 11198 | Watson GUP 11198 | Watson GUP 11198 |
| 7 | | | Watson GUP 11198 | Watson GUP 11198 | Watson GUP 11198 |
| 8 | 20 | | Watson GUP 11198 | Lesher GUP 11320 | Lesher GUP 11320 |
| 9 | | | Lesher GUP 11320 | Lesher GUP 11320 | Lesher GUP 11320 |
| 10 | | | Lesher GUP 11320 | | |
| 11 | | | | Lesher GUP 11320 | Lesher GUP 11320 |
| 12 | | | Lesher GUP 11320 | Lesher GUP 11320 | Lesher GUP 11320 |
| 13 | 21 | | Lesher GUP 11320 | LVP DDIA Setup | LVP DDIA Setup |
| 14 | 22 | | LVP DDIA Setup | Hilairet GUP 11166 | Hilairet GUP 11166 |
| 15 | | | Hilairet GUP 11166 | Hilairet GUP 11166 | Hilairet GUP 11166 |
| 16 | | | Hilairet GUP 11166 | Hilairet GUP 11166 | Hilairet GUP 11166 |
| 17 | | | Hilairet GUP 11166 | | |
| 18 | 23 | | | LVP DDIA Setup | LVP DDIA Setup |
| 19 | | | LVP DDIA Setup | LVP DDIA Setup | LVP DDIA Setup |
| 20 | 24 | | LVP DDIA Setup | Y. Wang GUP 11160 | Y. Wang GUP 11160 |
| 21 | | | Y. Wang GUP 11160 | Y. Wang GUP 11160 | Y. Wang GUP 11160 |
| 22 | | | Y. Wang GUP 11160 | Y. Wang GUP 11160 | Y. Wang GUP 11160 |
| 23 | | | Y. Wang GUP 11160 | | |
| 24 | | | | | |
| 25 | 25 | XAFS | | XAFS Setup | XAFS Setup |
| 26 | 26 | | XAFS Setup | Lindsay GUP 10199 | Lindsay GUP 10199 |
| 27 | | | Lindsay GUP 10199 | Lindsay GUP 10199 | Lindsay GUP 10199 |
| 28 | 27 | | Lindsay GUP 10199 | Gibson GUP 10444 | Gibson GUP 10444 |
| 29 | | | Gibson GUP 10444 | Gibson GUP 10444 | Gibson GUP 10444 |
| 30 | | | Gibson GUP 10444 | Gibson GUP 10444 | Gibson GUP 10444 |
| 31 | | | Gibson GUP 10444 | | |

## April

| Date | ESAF | Tech | 00:00 - 08:00 | 08:00 - 16:00 | 16:00 - 24:00 |
|---|---|---|---|---|---|
| 1 | 28 | | | Behrends GUP 9160 | Behrends GUP 9160 |
| 2 | | | Behrends GUP 9160 | Behrends GUP 9160 | Behrends GUP 9160 |
| 3 | | | Behrends GUP 9160 | Behrends GUP 9160 | Behrends GUP 9160 |
| 4 | 29 | | Behrends GUP 9160 | Beak GUP 11314 | Beak GUP 11314 |
| 5 | | | Beak GUP 11314 | Beak GUP 11314 | Beak GUP 11314 |
| 6 | | | Beak GUP 11314 | Beak GUP 11314 | Beak GUP 11314 |
| 7 | | | Beak GUP 11314 | | |
| 8 | 30 | | | Hettiarachchi GUP 11342 | Hettiarachchi GUP 11342 |
| 9 | | | Hettiarachchi GUP 11342 | Hettiarachchi GUP 11342 | Hettiarachchi GUP 11342 |
| 10 | | | Hettiarachchi GUP 11342 | Hettiarachchi GUP 11342 | Hettiarachchi GUP 11342 |
| 11 | 31 | | Hettiarachchi GUP 11342 | Dargaud GUP 11270 | Dargaud GUP 11270 |
| 12 | | | Dargaud GUP 11270 | Dargaud GUP 11270 | Dargaud GUP 11270 |
| 13 | | | Dargaud GUP 11270 | Dargaud GUP 11270 | Dargaud GUP 11270 |
| 14 | | | Dargaud GUP 11270 | | |
| 15 | 32 | | | Thayaril GUP 10449 | Thayaril GUP 10449 |
| 16 | | | Thayaril GUP 10449 | Thayaril GUP 10449 | Thayaril GUP 10449 |
| 17 | | | Thayaril GUP 10449 | Thayaril GUP 10449 | Thayaril GUP 10449 |
| 18 | 33 | | Thayaril GUP 10449 | Gerson GUP 9082 | Gerson GUP 9082 |
| 19 | | | Gerson GUP 9082 | Gerson GUP 9082 | Gerson GUP 9082 |
| 20 | 34 | | Gerson GUP 9082 | Schijf GUP 8463 | Schijf GUP 8463 |
| 21 | | | Schijf GUP 8463 | Schijf GUP 8463 | Schijf GUP 8463 |
| 22 | | | Schijf GUP 8463 | | |
| 23 | | | | | |
| 24 | | | | | |
| 25 | | | | | |
| 26 | | | | | |
| 27 | | | | | |
| 28 | | | | | |
| 29 | | | | | |
| 30 | | | | | |

# GSECARS Past and Present

Yongseong Choi
Przemyslaw Dera
Peter Eng
Sanjit Ghose
Nadege Hilairet
Anastasia Kantor
Innokenty Kantor
Atsushi Kubo
Ellen LaRue
Barbara Lavina
Nancy Lazarz
Matt Newville
Joe Pluth
Vitali Prakapenka
Clayton Pullins
Mark Rivers
Takeshi Sanehira
Fred Sopron
Steve Sutton
Tom Trainor
Yanbin Wang

Visit: www.cars.uchicago.edu